

**Computer Science Department Technical Report
University of California
Los Angeles, CA 90024-1596**

**NEURAL NETWORK MODELS OF ILLUSORY CONTOUR
PERCEPTION**

B. Ringer

**December 1992
CSD-920056**

UNIVERSITY OF CALIFORNIA

Los Angeles

**Neural Network Models of Illusory Contour
Perception**

A thesis submitted in partial satisfaction
of the requirements for the degree
Master of Science in Computer Science

by

Brian Ringer

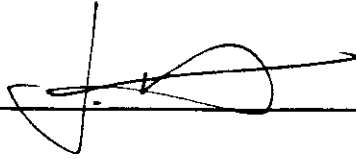
1992

© Copyright by

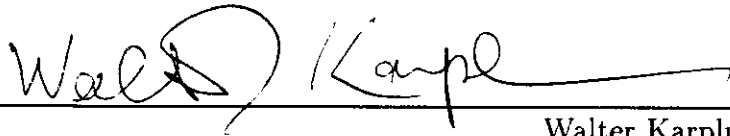
Brian Ringer

1992

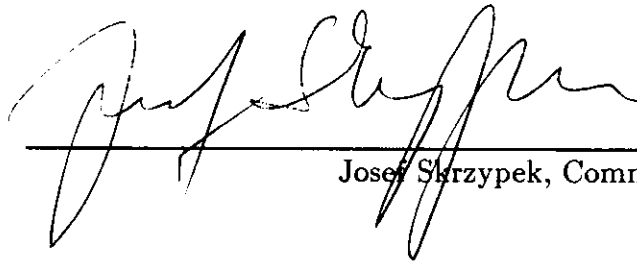
The thesis of Brian Ringer is approved.



Jacques Vidal



Walter Karplus



Josef Skrzypek, Committee Chair

University of California, Los Angeles

1992

TABLE OF CONTENTS

1	Introduction	1
1.1	Illusory Contours	2
1.2	Psychophysics	5
1.2.1	Depth Effects	6
1.2.2	Surface Brightness	6
1.2.3	Oriented Contour Perception	7
1.2.4	Interaction with Perceptual Primitives	8
1.2.5	Higher Level Interactions	8
1.3	Physiology	11
1.4	Illusory Contours and Visual Perception	13
2	Theories and Models of Illusory Contour Perception	16
2.1	Cognitive Models	16
2.1.1	Gestalt of the Form	16
2.1.2	Occlusion	18
2.2	Computational Models	19
2.2.1	Brightness Contrast	19
2.2.2	Locality Conjecture	20
2.2.3	Nonlinear Summation	20
2.2.4	Recurrent Networks	21

2.2.5	Contour Neurons	21
2.2.6	Snakes	22
2.2.7	Gestalt Groupings	22
2.2.8	Feature Groupings	23
2.2.9	Reentrant Processing	24
2.2.10	Evidence Summation	24
2.3	General Contour Neurons	31
3	Computational Model	35
3.1	Feedforward Component	38
3.2	Recurrent Component	44
3.3	General Contour Neuron	46
4	Simulation Results	50
4.1	Methods	50
4.2	Results	54
5	Discussion	64
5.1	Oriented Contour Perception	65
5.2	Depth Perception	65
5.3	Brightness Perception	66
5.4	Anatomical Considerations	67
5.5	Future Work	70
5.6	Conclusions	71

References 73

LIST OF FIGURES

1.1	Perception and recognition is still possible in the absence of boundary information. (a) An object whose boundaries are partially occluded by other objects. (b) The boundaries of the object are not well represented as continuous discontinuities. The object can still be identified (after Ramachandran, 1988).	2
1.2	Examples of illusory contours.	4
1.3	An illusory triangle can be seen with some effort among the incomplete elements (after Coren, 86).	10
2.1	(a) An illusory surface occluding several other objects. (b) When the background elements are replaced by fragments instead of complete objects, the perceptual strength of the illusory contours is not diminished.	17
2.2	Illusory surfaces induce a distinct perception of depth. Here, the assignment in depth of the illusory triangle alters the perception of the relative sizes of the two identical circles.	18
2.3	(a) A bright illusory bar is seemingly induced by the dark image elements. (b) The perceptual salience of the illusory bar is not reduced when the contrast of the inducing elements is sharply reduced.	19
2.4	The geometry of the (ρ, θ) transformation.	25

2.5	The enhanced Hough transform network. Edges are detected from the image, and then compete using a winner-take-all mechanism. Remaining points vote for lines passing through them using orientation and offset information. Evidence layers are recombined to yield all lines present in the image.	27
2.6	(a) An input image showing the broken outline of a figure. (b) The network was able to detect lines corresponding to the complete boundary of the figure despite gaps in the border.	29
2.7	(a) An illusory bar can be seen occluding the broken rectangles. (b) Lines detected correspond to both normal contours and to the boundaries of the illusory surface.	30
2.8	(a) A cluttered gray level image, and (b) The lines detected by the Hough transform network.	31
2.9	(a) An input image containing an illusory bar. (b) In cases where the illusory contour was orthogonal to the inducing segments the network had a tendency to make the amodal completions	32
2.10	Minimal alteration of the image intensity profile in regions spatially separated from the “gaps” dramatically alters the saliency of the illusory contours perceived.	34
3.1	The General Contour Neuron. The cell receives input from two parallel sub-systems: luminance edges and illusory contours. The illusory contour component is driven by summation of orthogonally oriented endstopped cells. Recurrent excitation modulates the response of the cell to the grouping inputs.	37

3.2	Network architecture	39
3.3	The receptive field profile of line termination groupings for (a) a GCN detecting a straight illusory contour, and (b) a GCN tuned to the detection of a right angle corner. Each pools asymmetrical hypercomplex cell responses consistent with the relative position of the occluding surface.	43
3.4	The diffusion process. Activity levels are communicated through connections between cells across the layer. Each cell connects to its 8 immediate neighbors. Activation levels spread through the cellular network until a steady state is achieved.	47
4.1	Full network simulation outputs with an illusory bar.	56
4.2	Possible contour completions based on line terminations with an illusory bar image. The General Contour Model makes only completions A & B, in correspondence with human psychophysics. Completions C, D, E & F are suppressed due to lack of recurrent excitation from surface neurons.	57
4.3	Full network simulation outputs with illusory square.	58
4.4	Simulation results for an abutting grating stimuli.	60
4.5	Simulation results for an elongated illusory bar.	60
4.6	Simulation results for a Kanizsa triangle.	61
4.7	Simulation results for a illusory rectangle given by opposite contrast polarity inducers.	61
4.8	Simulation results for a modified sun illusion.	62

4.9	Simulation results for overlapping surfaces.	62
4.10	Simulation results for a discontinuity impaired image.	63
5.1	Speculative anatomical correlates of illusory contour processing by the primate visual system.	68

LIST OF TABLES

4.1	The parameters used in the network.	52
4.2	Additional parameters used in the network.	53

ACKNOWLEDGMENTS

I would like to thank the following for their invaluable assistance over the last few years: Professor Josef Skrzypek, my esteemed advisor; Edmond “the basketball master” Mesrobian, David Gungner, George Wu, Dr. Michael D. Stiber and the rest of the mpl dancing dunces; David Gast, Dinh Le, Ron Sumida, Trent Lange, Matthew Merzbacher, Moises Goldszmidt, Ed Praitis and my many other fellow graduate students; Andy Jacobson, Bill Clinton, Charles Barkley, Dave Thau, the Dead Kennedys, Jerry Brown, Jon Khatt, Kim Po, Mario Escamilla, Mark Schaefer, Raquel Rivero, Ted Koppel and Todd Hendrix for their generous monetary contributions to my cause; the entire Phlegm Cocktail team and all the various riff-raff who I’ve dunked over on the courts; all the late night burrito stands in Los Angeles; the people at Perceptronics and MSI for helping keep me off the streets; Steven, Karen, Will, Michelle, Arron, Kathy and my other poignant and pensive siblings; and most importantly, my Mom and Dad for the patience and support to allow me to pursue this degree.

ABSTRACT OF THE THESIS

Neural Network Models of Illusory Contour Perception

by

Brian Ringer

Master of Science in Computer Science

University of California, Los Angeles, 1992

Professor Josef Skrzypek, Chair

Illusory contours result from occlusion by a surface whose border is not defined by a continuous discontinuity in any image attribute. This thesis presents a computational model of illusory contour processing based on a neural architecture which aggregates boundary and surface information. Ambiguous completions of illusory contours are resolved through recurrent interactions between contrast sensitive cells, hypercomplex cells and hypothesized surface neurons which combine information from spatially separated contour features defining visual surfaces. Computer simulation results demonstrate that the model can extract all perceptually salient contours in a variety of well known illusory contour patterns. Furthermore, the model explains the three major perceptual effects associated with illusory contours: oriented contour perception, depth effects and increased brightness.

CHAPTER 1

Introduction

The primary goal of a vision system is to provide an interpretation of a surrounding scene. Crucial to this process is finding the boundaries of the surfaces and objects which make up the scene. Typical computer vision algorithms approach this by finding discontinuities in one or more image attributes, for example brightness, color, motion and depth [Hor86]. However, these algorithms frequently fail in segmentation of images from unconstrained environments because all object boundaries are not well represented as such discontinuities. Confounding elements include shadows and shading, uneven lighting and partial occlusions by other objects. And yet, examples of human perception and recognition of objects with missing data are widespread: objects are easily recognized despite being partially occluded by other surfaces or objects (Fig. 1.1). Further, boundaries which are not well defined as image discontinuities often do not prevent object segmentation and identification (Fig. 1.1).

Examples such as these suggest that in human vision relatively little physical data is needed in order to create a percept; “making up” missing information seems to be a routine process. Evidence of similar processes are widespread, for example the perceptual filling-in of retinal scotomas [RG91, PN91]. Here, the path of the optic nerve prevents any retinal activity in a small area of the visual field. Information from nearby areas is filled-in over this region to maintain

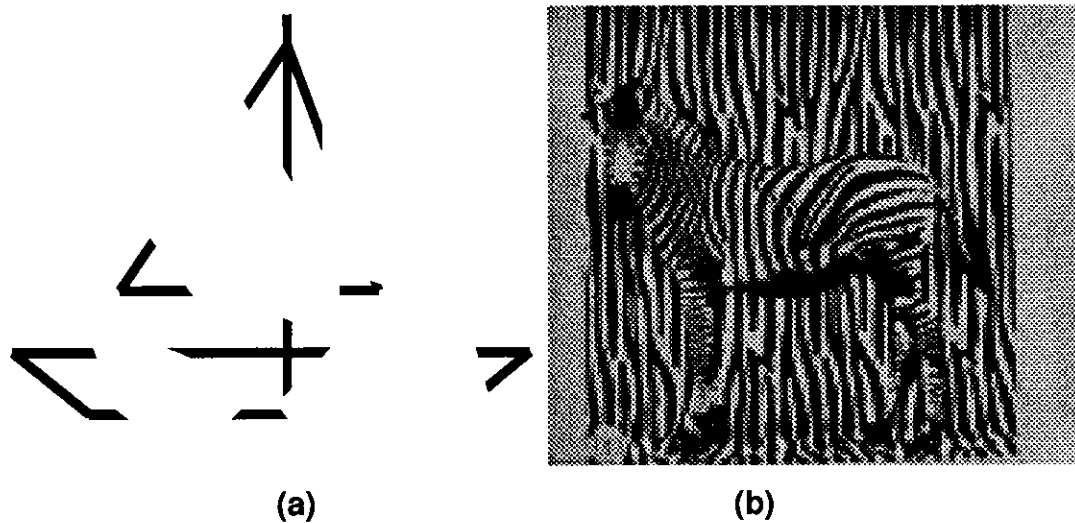


Figure 1.1: Perception and recognition is still possible in the absence of boundary information. (a) An object whose boundaries are partially occluded by other objects. (b) The boundaries of the object are not well represented as continuous discontinuities. The object can still be identified (after Ramachandran, 1988).

consistency of perception. The missing information may be filled-in to maintain consistency with previously defined goals and expectations, based on past visual experience. Apparently the visual system tries to arrive at a meaningful interpretation of a scene even by imposition of subjective expectations and assumptions on the actual reality of the visual sensation.

1.1 Illusory Contours

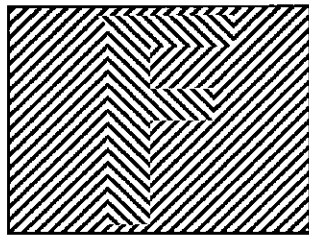
In attempting to provide accurate segmentation of a scene the human visual system uses many clever techniques [Ram85b]. Although visual primitives such as brightness, color and texture typically vary at object boundaries, they can often be uniform between neighboring objects, or vary on the surface of an object

(such as the striped surface of a zebra). Depth boundaries however have a higher correspondence to actual object boundaries [NSS89]. A typical visual scene contains many partially overlapping surfaces. Thus it would be advantageous to have visual mechanisms tuned specifically to the detection of overlapping surface boundaries (occluding contours). Such a mechanism may exist in humans (as well as other mammals [BBM88, RCC86, HPB84]) as evidenced by their ability to perceive illusory contours ¹.

Illusory contours are boundaries of perceptually occluding surfaces which are not defined by any physical luminance discontinuity (see Fig. 1.2 for several examples). Instead, the contour is perceptually induced by alignments of visual cues which signal occlusion, such as sudden terminations of background structure, as typified by line endings or corners. The human visual system is able to fill-in an occluding contour using only a limited amount of visual data. In real world situations aligned discontinuities have a high level of coexistence with occluding contours, thus through evolution and visual experience they have become linked in the human visual system [PSN89]. Such an approach appears to be quite efficient; direct estimates of occluding boundaries, and thus of surface position and extent, can be obtained through detection of a few key points, without having to undergo the computational burden of processing the vast amounts of visual information present. Thus, the laboratory phenomenon marked by the perception of “phantom” contours may in fact be an artifact of a powerful visual mechanism used to rapidly compute depth segmentations.

Illusory contours as a perceptual phenomenon have been documented as far

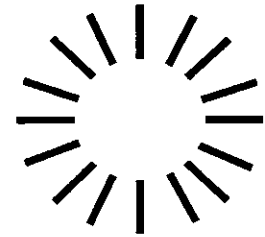
¹Illusory contours have variously been called by many names, subjective or anomalous being the two most commonly used others. The term illusory contours will be used throughout this thesis.



(a)



(b)



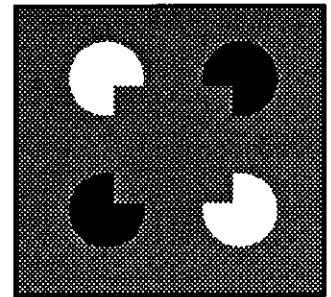
(c)



(d)



(e)



(f)

Figure 1.2: Examples of illusory contours.

back as 1904 with Schumann's work on contours perceived at broken intersections points in a grid [Sch04]. They were first brought to widespread attention by Kanizsa [Kan54, Kan76], who demonstrated the power and flexibility of illusory contours perception. Psychophysical research into illusory contours and their role and visual perception increased through the 70's and early 80's (see [PC92b] for an illustration of the dramatic rise in interest). In 1984 the first direct physiological correlates to the perception were revealed by neuronal responses in early layers of the monkey visual cortex to stimuli which induced the perception of an illusory contour in humans [HPB84]. These results spurred a new wave of analysis of illusory contours, increasingly focused on defining the functional specifications of the perception [Pra85, SG85, Ram86, PSN89]. Illusory contours have now been implicated in the perception of camouflaged objects [Ram86], contrast detection [SK90], figure/ground discrimination [Kan76], surface depth determination [Cor72] and others. As their role in visual form perception becomes more apparent, illusory contours beginning to be addressed increasingly in computational models of vision [GM85, KWT87, FE89, McC90, SR92a].

1.2 Psychophysics

The psychophysical aspects of illusory perception have been studied extensively over recent years (see [PM87] for a review). These experiments have shown the ability to perceive illusory contours is extremely robust across human observers; psychophysical experiments with illusory contours are repeatable and consistent. Further, various experiments have shown that illusory contours are perceived by other animals as well; confirmation exists for cats [BBM88] and evidence has been advanced for primates as well [HPB84]. The major psychophysical elements of

illusory contour perception are detailed below.

1.2.1 Depth Effects

Illusory surfaces are usually accompanied by a strong impression of a perceptual depth discontinuity [Cor72]. The illusory surface seems to be nearer in depth than the background elements, corresponding to the location of an actual occluding surface overlaying the background elements. Although there are cases where this depth impression is reduced [Ken78], it is typically a fairly vivid and robust companion of the perception of an illusory surface.

Further psychophysical experiments have illuminated the relationship between illusory contours and depth. Experiments where stereoscopic depth information is presented which is incompatible with the perception of an occluding surface (ie. placing the illusory surface in the far disparity plane) reduces or removes the perception of the illusory contour [GH74]. There is a striking perceptual similarity between illusory contours and other types of phantom contours generated by direct manipulation of depth cues. The boundaries of surfaces offset in depth by manipulation of stereoscopic information in random dot stereograms are perceptually similar to illusory contours [Jul71]. Similar contours are seen bounding surfaces which arise from stereoscopic images with unpaired image points (so called Da Vinci occlusion) [NS90].

1.2.2 Surface Brightness

Illusory surfaces appear brighter than their backgrounds, even when the two are stimulus identical [Kan76]. For example, a white illusory surface given by black inducing elements will appear to be noticeably brighter than the background (see

Fig. 1.2). The increased brightness is dependent on perception of the illusory contour themselves, and varies with the strength of the illusory percept. Elements which effect this perceptual strength, such as contrast and proximity of the inducing elements, effects the perceived brightness difference [DLB90]. This enhancement may be merely an artifact of the normal brightness enhancement which occurs when an object is perceived as a “figure” [Par89], although the effect seems to be stronger than usual with illusory surfaces. An interesting case is presented by illusory contours defined by opposite polarity brightness contrast inducers [SG87]. Here the alteration in surface brightness is much perceptibly reduced and non-uniform (Fig. 1.2).

1.2.3 Oriented Contour Perception

Illusory contours are perceived as very real, salient contours. Results have shown that the human visual system has the ability to discriminate the orientation of an illusory contour at levels approaching those of regular contours [VO87]. Further, there is an interaction between illusory contour and real contour orientation discrimination abilities; practice with illusory contours increased ability with normal contours, suggesting that illusory and real contours may be at least partially processed by the same visual mechanisms.

Illusory contours have been shown to induce tilt aftereffects (the alteration of perceived orientation through the repeated presentation of differently oriented stimuli) similar to those perceived with normal contours [SO75, PSN89]. Furthermore, interocular exchange of these aftereffects has been reported [PSN89]. This suggests that illusory contours are processed at binocular neurons, consistent with the interaction between illusory contours and depth.

Research on the necessary conditions for the perception revealed evidence which supports the extraction of illusory contours by early feature detection type mechanisms. Completion of contour, although influenced by many factors, requires the presence of sharp discontinuity information (a discontinuity in the first derivative of the luminance profile) [SK90]. Psychophysical data has also shown that there exists a maximum sized gap that can be perceptually crossed by the contour [SG85]; the size is dependent upon retinal position of the contour, increasing from a value of roughly 0.5 visual degrees in the fovea to a maximum of almost 2° in the periphery. This fixed size can be correlated with a visual receptive field size.

1.2.4 Interaction with Perceptual Primitives

Illusory surfaces exhibit many of the same properties as normal surfaces, such as stereo and motion capture [Ram85a]. Furthermore, illusory contours disappear at isoluminance; they cannot be generated by inducers which are defined only through non-luminance based cues, such as isoluminant textures [Ram86], isoluminant colors [Ram86], stereopsis [Pra85] or flicker [Pra85]. This failure of clearly perceptible inducers to generate illusory contours suggests that the perception might lie with an early luminance based visual mechanism.

1.2.5 Higher Level Interactions

Many experiments have demonstrated that higher level, “cognitive” variables, if not entirely responsible for illusory contour perception, at least have an impact upon it. This is supported by the claim that illusory surfaces are perceived only when they occlude figures which by themselves are not globally complete [Kan76].

A simple demonstration of this is a white square occluding one quadrant of a circle. Our assumption that the occluded object is a circle fulfills the requirements of Gestalt principles; if parts of a form appear to be incomplete, an illusory contour will result.

Additional evidence of high level interactions comes from results showing that some illusory contours are not always immediately perceived. In noisy patterns containing illusory surfaces, often the surface is not perceived until the pattern is studied for a while, or the figure is pointed out to the observer, after which the illusory surface is consistently perceived [CPT86] (see Fig. 1.3). Further, the time to perception of some contours is dependent upon the perceptual set of the viewer.

Other work has similarly demonstrated that illusory contour perception may not be totally dependent on luminance stimulus array [BD75]. In figures involving multiple illusory figures, which illusory contours are perceived can be modified by what the observer is directed to see. However, in these examples, the different sets of illusory contours were usually in competition with each other; perceiving one set of contours makes the other perceptually impossible (for example because of incompatible depth assignments). The varying perceptions in these cases may have the same origins as other examples of perceptual selection, for example the Necker cube or Rubin's famous faces/vases displays [Rub58].

The role of memory in the perception of illusory contours has been addressed, with some results to support the claim that familiarity can increase the ability to perceive the illusory surface [WS88]. However, the many examples of perception of arbitrary irregular shapes [Kan76] indicates that familiarity with the object defined by illusory contours is not a necessary precondition for the perception.

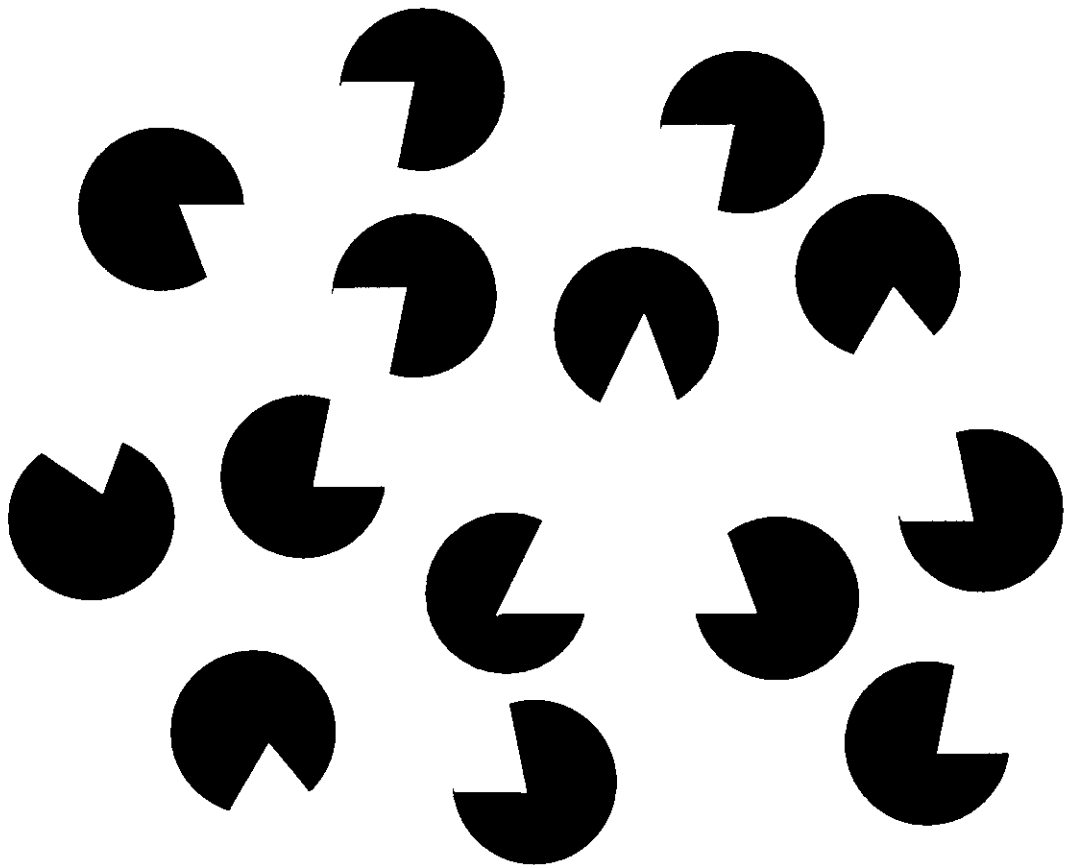


Figure 1.3: An illusory triangle can be seen with some effort among the incomplete elements (after Coren, 86).

1.3 Physiology

Illusory contour perception has been studied physiologically as well as psychophysically. Experiments with both monkeys and cats revealed neuronal responses to stimuli which induce the perception of an illusory contour in humans [RCC86, HPB84]. These results have contributed greatly to understanding the manner in which illusory contours are processed in biological vision systems.

The widest body of evidence comes from experiments conducted by R. von der Heydt, E. Peterhans and G. Baumgartner which demonstrated responses to illusory contour stimuli in visual area V2 (pre-striate cortex) of alert, fixating rhesus monkeys [HPB84, PH89, HP89]. While the monkeys performed a visual discrimination task, simple illusory contour patterns (a thin illusory bar, and an illusory grating border (see Fig. 1.2) were presented, and cells in areas V1 and V2 were recorded from. Of cells which responded to the orientation contrast boundary, roughly 40% in area V2 also responded to illusory contour stimuli. No cells in area V1 responded to illusory contours. The strength of the relative responses were found to vary widely from cell to cell, with either the illusory contour or the real contour response being dominant, to all levels in between. Orientation and directional selectivity were roughly equivalent for both types of contour. The effects of perceptual set and attention were not measured in the experiments so these factors cannot be discounted or affirmed. No attempt was made to classify the cells into traditional hierarchies (simple, complex, etc.), although it was noted that all identified cells were binocularly driven.

Alterations in the visual stimuli used in the experiments helped to further illuminate the nature of the cellular responses [PH89, HP89]. For abutting grating stimuli, experiments measured responses to variables such as number and phase of

the line segment endings and overlap/separation of the two regions. The resulting responses showed a high degree of correlation with the perceptual strength of the induced contour. Responses gradually increased with the number of line segments, with a minimum of 4 or 5 lines to produce a response and reaching a peak thresholded response at about 10 inducing lines. Altering the orientation of the line segments away from the orthogonal to the contour lowered the response. The distance between the segments was shown to be very important. Maximum response was obtained with small gaps (.2 visual degrees) and deteriorated until crossing a threshold ($\approx 1.6^\circ$ but varying from cell to cell). In situations where either half of the grating was presented without the other half no substantial response was obtained.

Experiments involving an illusory bar (Fig. 1.2) showed similar response dependence on perceptual salience. If the bar gap became too wide, above some cellularly dependent threshold, the response was extinguished. If either one of the inducing sections were removed the response was extinguished. When the bar sections were “closed”, meaning that small connecting lines were drawn across the open end of the bar, the responses were also extinguished, in accordance with human perception. Interestingly, cellular response levels for illusory bars were typically much higher than would be predicted from the number of line segments present obtained from abutting gratings. This seems to indicate that the cellular response was dependent on more than just a simple summation of line endings.

Cells sensitive to illusory contours were reported in areas 17, 18 and the dorsal lateral geniculate nucleus of anesthetized cats [RCC86]. Stimuli used were illusory contours generated by abutting gratings. As with monkeys, the cellular responses varying with perceptual salience of the stimuli. The differences of these

results with data from monkeys could be due to a number of reasons: the neuronal organization differences between monkeys and cats, the use of anesthetized versus alert subjects, or differences in recording procedure.

Lastly, preliminary results have been reported by Robert Shapley suggesting that some illusory contours may be signaled by neurons in area V1 of the monkey visual cortex. The stimuli used were very dense groups of lines, similar to abutting gratings, which produce an illusory contour at their endings. This data has yet to be formally published, so no attempts at analysis of these results within the context of other physiological data can be made.

All of these results suggest that illusory contour perception is at least partially determined at early layers of visual processing. Feedback from higher cognitive layers cannot be ruled out completely, but cellular response times are short enough to seemingly rule out complex feedback processes. Further, the graded response levels corresponding to perceptual strength of the contour argues against a cognitive “decision making” process.

1.4 Illusory Contours and Visual Perception

Recent visual theories have suggested that much of what is perceived is based on limited data, which is then filled-in to arrive at a stable perception [RG91, PN91, SG92]. Further, there has been speculation that human vision may use a variety of special purpose “tricks” to rapidly solve problems which are too computationally demanding to solve directly. For example, work by V.S. Ramachandran showed that when computing surface profiles from shading information, the human visual system uses the assumption that the light source (presumably the sun) is always directly above the head [Ram86]; this assumption is typically valid

as humans spend the bulk of their time upright and removes the computational burden of having to constantly recompute the position of the light source for even rapid recognition. Illusory contours may be the result of a special purpose visual mechanism used to detect occlusions based on cues which typically signal the boundary of an overlapping surface. Once the occluding contour is signaled, the surface and perceptual contour can be filled-in by active visual processes. Following these examples may provide artificial vision systems with solutions to problems which are computationally too expensive when using standard techniques [PTK85].

The physiological data reported strongly suggest that illusory contours are a fundamental perceptual primitive used by biological systems in image segmentation; to have such a large percentage of cells triggered by illusory contour stimuli seems to indicate visual mechanisms specifically tuned to detect these types of occlusion. The manner in which illusory contours are processed by biological vision systems will probably illuminate many organizational principals of these systems. Further, illusory contours represent a unique perceptual phenomenon touching directly into issues such as form perception, filling-in, and integration of top-down and bottom-up information among others. Lastly, a solution to illusory contours may be part of a larger solution to occluding surface segmentation, particularly in data impaired situations. Understanding such mechanisms would be of enormous benefit for construction of artificial vision systems operating in unconstrained environments.

However, the diversity of the psychophysical and physiological data makes it difficult to evaluate hypothesized explanations without computational models enforcing explicitness of constraints and assumptions. The objective of this

thesis is to introduce a computational model of the neural structures underlying illusory contours and to examine in depth the compatibility between physiological, computational and psychological theories. A computational model of illusory contour perception is described based on available anatomical, physiological and psychophysical data. This model is then implemented as a neural network, and simulation results presented showing that the network has the ability to detect illusory contours in a wide variety of images.

CHAPTER 2

Theories and Models of Illusory Contour Perception

The wealth of available psychophysical and physiological data has produced many theories and models of how illusory contours are processed by the human visual system. These theories can be roughly broken into two broad categories: those which attribute the major cause of illusory contour perception to cognitive top-down processing, and those which opt instead for a bottom-up, computational type approach. As with any classification system, there is not always a clear boundary or grouping for each theory, and many theories and models take a little from each category. The major proponents of each group as well as their relative strengths and weaknesses will be discussed here. Finally, a computational model of illusory contour perception will be described which is the focus of this thesis.

2.1 Cognitive Models

2.1.1 Gestalt of the Form

The most popular cognitive model attributes illusory contours to the Gestalt Principles of form perception [Kan76]. Here, subjective contours result from the prerogative of the visual system to perceive forms. Good form perception is guided by Gestalt Principles including symmetry, regularity, closure and simplic-



Figure 2.1: (a) An illusory surface occluding several other objects. (b) When the background elements are replaced by fragments instead of complete objects, the perceptual strength of the illusory contours is not diminished.

ity. Kanizsa differentiates between forms that arise from physical sensory data and forms that are perceived because we have knowledge of them in absence of complete sensory input. The latter case applies to forms that are occluded or arise from perception of occluding surface, and can be explained in terms of an unconscious inference made on the part of the perceiver. The visual system, in attempting to observe the Gestalt rules of object formation arrives at a perception involving illusory contours. Thus, illusory surfaces would be perceived only when they occlude figures which by themselves are not globally complete [Kan76]. A simple demonstration of this is a white square occluding one quadrant of a circle. Our assumption that the occluded object is a circle fulfills the requirements of Gestalt principles; if parts of a form appear to be incomplete, an illusory contour will result. However, through rigid experimentation, counterexamples have been found showing that even with properly aligned “complete” elements, illusory contours can still be weakly perceived [DK83]. Another example challenging this hypothesis is shown in Fig. 2.1; here the perceptual strength of the contours is not diminished by the removal of possible amodal completions.

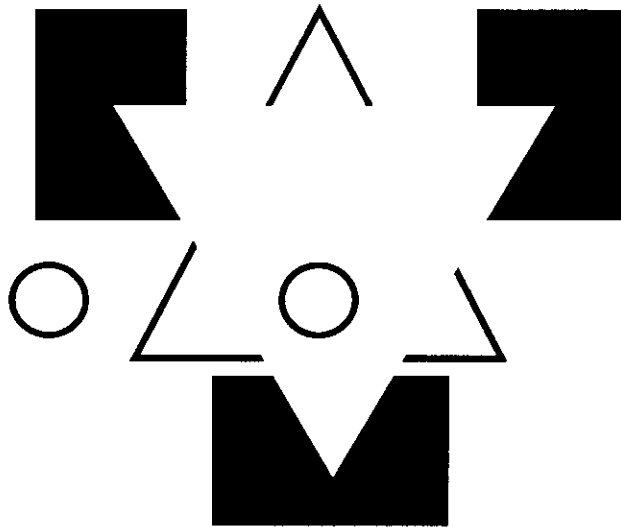


Figure 2.2: Illusory surfaces induce a distinct perception of depth. Here, the assignment in depth of the illusory triangle alters the perception of the relative sizes of the two identical circles.

2.1.2 Occlusion

Depth information and perception of occluding surfaces has been suggested as an explanation of subjective contours [Cor72]. In many examples this hypothesis seems to be valid; illusory contours arise from edges of surfaces that occlude real objects. The relationship between the judgement of apparent depth and an illusory contour is best demonstrated in Fig. 2.2. Two circles subtended by the same arc appear to be of different size; one placed on top of the perceived triangle seems to be smaller due to the apparent nearness of the subjective triangular surface. In some sense the occlusion and apparent depth hypothesis of Coren could be subsumed by Kanizsa's explanation: apparent surfaces in the foreground result from the incompleteness of the background.

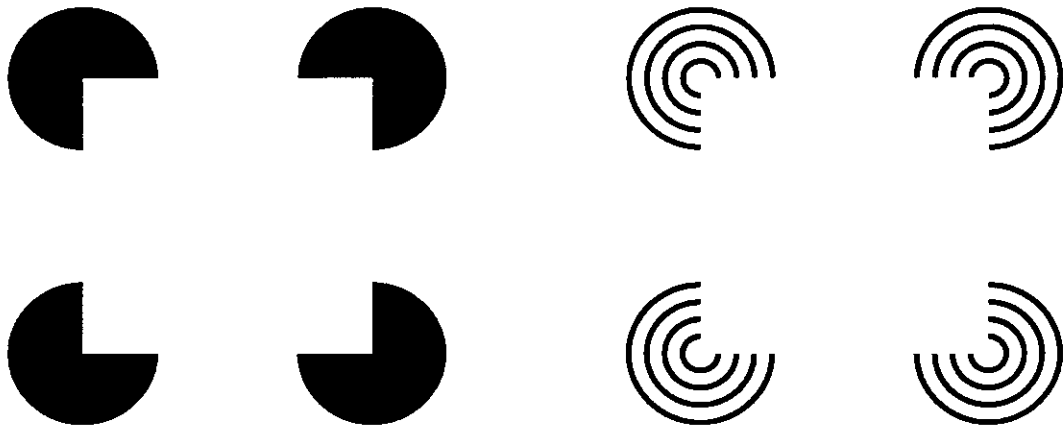


Figure 2.3: (a) A bright illusory bar is seemingly induced by the dark image elements. (b) The perceptual salience of the illusory bar is not reduced when the contrast of the inducing elements is sharply reduced.

2.2 Computational Models

2.2.1 Brightness Contrast

One conjecture about the appearance of subjective surface is based on apparent brightness contrast in the real image (Fig. 2.3(a)) [FC75]. Here, the bright illusory bar seems to be induced by the dark edges of all figures “occluded” by the bar; the contours seem to be especially vivid where boundaries of the occluded surfaces are represented by many points of discontinuous contrast. Mechanisms similar to early visual spatial filtering could predict the presence of the illusory contour [Gin75]. However, counter examples have been shown where very little brightness contrast is needed to generate an illusory percept, invalidating this theory (Fig. 2.3(b)).

2.2.2 Locality Conjecture

Ullman has suggested that illusory contours may result from real boundaries which can be extended to produce a subjective contour by local operations [Ull76]. Although this proposal is devoid of direct physiological support, it suggests that a network could fill the gaps in a contour. Multiple layers of orientation detectors receive data from a fixed range of orientations and contribute laterally to neighboring neurons that are collinear with the center of the input range. Thus gaps between edge segments would induce minimum curvature connections, resulting in a global filling-in effect. This is analogous to fitting a curve with cubic splines. However, counterexamples have been found [Kan79] (Fig. 1.2), where subjective contours do not lie along the same direction as the real edges in the image and in fact can be perpendicular.

2.2.3 Nonlinear Summation

The illusory contour detection process appears to be nonlinear. Arrangement of pattern elements and cues outside of a cell's normally defined receptive field can induce a response across a physically homogeneous area. A simple nonlinear summation mechanism to account for these illusory percepts has been proposed by Shapley and Gordon [SG85]. The mechanism gates edge responses (of possibly opposite polarity) across a fixed sized gap, resulting in completion of the border. Similar to Ullman's model, the orientation of the illusory contour must be coincidental with the edge pieces generating it. However, the model will complete illusory contours across arbitrary gaps, possibly contradicting human psychophysical performance.

2.2.4 Recurrent Networks

Grossberg and Mignolla suggested that a computational model loosely based on the organization of early layers of the primate visual system could account for illusory contour perception [GM85]. Their model is characterized by interactions between a boundary contour system (BCS) which produces the edges of objects, and a feature contour system (FCS) which fills in interior information. The BCS is a cooperative/competitive circuit which uses recurrent iterations to complete broken or fragmented outlines, based on the output of oriented edge filters (complex cells). Line segments of similar orientation cooperate through a spatially long range process to produce boundary completion. Line endings induce small segments oriented orthogonally to the inducing segment. These small induced segments can cooperate spatially to form a complete boundary. Pieces of the boundary feedback through the competitive loop, producing a relaxation effect between different border pieces which helps to eliminate spurious segments. Simulations of the BCS were reported suggesting its ability to fill in a fragmented borders, as well as detect a limited subset of illusory contours [AK87]. However, as the model relies solely on local luminance information to complete an illusory contour, gaps between arbitrarily aligned segments which do not belong to the same object are often completed.

2.2.5 Contour Neurons

R. Von der Heydt and E. Peterhans proposed a neural mechanism to explain their recorded responses from cells in monkey visual cortex to illusory contour stimuli [PHB86]. They suggest that a subset of cells called “contour neurons” exist in area V2 which respond to both real and illusory contours. Each of these

neurons sums two inputs originating in area V1; the first corresponds to oriented luminance gradient contours. The second is based on occlusion cues, orthogonal aligned discontinuities, detected by hypercomplex cells with asymmetrical end inhibition. Such cells are thought to detect end points, curvature and corners [KNM84, DZC87, VOL90, WR89, HRH92]. Orthogonal hypercomplex cell outputs are summed across the gap spanned by the illusory contour. This model is the first attempt to explain illusory contour perception in terms of known physiological and anatomical organizations of the visual cortex.

2.2.6 Snakes

A similar method of perceptual grouping which incorporates a method for orthogonally oriented completion is described by the “snakes” model [KWT87]. Here, an energy minimizing contour spline (the snake) is fitted to low-level image features such as edges or line endings. The fit can be controlled by the influence of different image features and other constraints through the manipulation of constants in an energy equation. Illusory contours can be detected by placing increased importance on line terminations and edge segments as image features. However, an initial high-level decision is needed to set the approximate position of the snake, and the model contains no method for automatically determining the relative importance of the various image cues.

2.2.7 Gestalt Groupings

A similar energy minimization framework can be used to control the grouping of tokens based on Gestalt laws of similarity, proximity, continuity, etc., [McC90]. A given scene may theoretically be interpreted (grouped) in many different ways.

However, one best interpretation needs to be selected, subject to criteria reflecting properties of the real world (the problem of ill-posedness of vision [PTK85]). One possible approach is to allow different local hypothesis to compete with each other. The competition can be realized by minimizing energy that reflects the intrinsic Gestalt property of each proposed grouping; tokens can be regrouped until a sufficiently low energy solution is obtained. However, choosing the proper energy functional to minimize the tokens to be grouped and the scale at which to allow interaction between tokens to occur remain open problems.

2.2.8 Feature Groupings

The grouping of orthogonally oriented line terminations to determine illusory contours has served as the basis for many more recent models. A recent effort by Manjunath and Chellappa proposes that illusory contours are detected as part of a hierarchical boundary detection scheme[MC91]. Here, orthogonally oriented line terminator information, along with edges and “textural” boundaries, are fed into a long range grouping mechanism. However, three immediate problems arise: 1) by not gating terminator information by similar activity on opposite sides of a gap, lines are completed stretching well passed their true end points, 2) the size of the grouping neighborhood must be set explicitly to allow detection of illusory contours as opposed to other types of contours, and 3) the network has difficulty detecting illusory contours marked by sparse line terminations, such as the Kanizsa triangle ???. Further, as with the models proposed by Grossberg and Shapley, no method for monitoring spurious responses is provided.

2.2.9 Reentrant Processing

A recent computational model by Finkel and Edelman proposes that illusory contours are completed as part of an occluding boundary detection process [FE89]. They construct a neural network which loosely parallels the functional anatomy of several cortical areas in the primate visual cortex. Illusory contours are completed by orthogonal line termination responses, subject to modulation by a reentrant signal (analogous to feedback between visual cortical areas). Additional constraints are placed on the completion process to suppress spurious responses; they require that contour completions have line terminations from both directions present. Although this allows some hypothetical completions between external object boundaries to be eliminated, the requirement seems overly restrictive. Many examples of illusory contours being completed between line terminations of the same direction are available in the literature (see Fig. 1.2(e)) and [Ken78].

2.2.10 Evidence Summation

The Hough transform provides a noise and occlusion insensitive technique for the detection of arbitrary analytic or non-analytic curves in an image [Hou62, DH72, Bal81]. This ability to function in cases of missing and limited data makes the Hough transform a potential model for illusory contour perception; a neural network implementation was simulated and evaluated as a computational model of illusory contour processing [RS91]. Image feature points “vote” for curves passing through them using a transformation to a parameter space. This space is then searched for evidence of the curves being detected. Thus, instead of fitting curves to data, a more tractable problem of detecting high density points in a parameter space is addressed. For example, a simple straight line parametrization

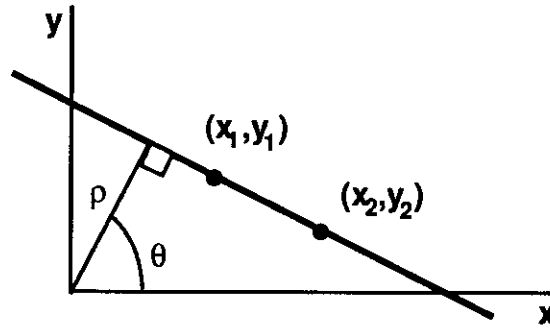


Figure 2.4: The geometry of the (ρ, θ) transformation.

is in terms of ρ , the perpendicular distance of the line from the origin, and θ , the angle of the normal to the line (see Fig. 2.4). Euclidean (x, y) coordinates are transformed into (ρ, θ) space by $\rho = x \cos \theta + y \sin \theta$.

Thresholded edge pixels are used as feature points; each increments a counter representing the (ρ, θ) parameters of all lines passing through the it. Thus, collinear edge points increment the same (ρ, θ) counter. Counters are stored in a two-dimensional accumulator array, which is thresholded to yield parameter combinations of high density, corresponding to lines present in the image.

Several modifications were made to the standard Hough transform model described above. First is the use of oriented edge information [Bal81]; this has the effect of uniquely constraining the set of lines passing through a feature point (θ becomes fixed). Further, edges are detected at a variety of spatial scales to ensure capturing all relevant edge information.

A well known problem of the Hough transform is its inability to localize detected curves (see [IK88]); detected lines span the entire image. To solve this problem, we allow edge points to vote for finite length lines spanning a local neighborhood centered at the edge position. This line length is fixed across all

spatial scales, and is typically in the range of 20 pixels in the simulations presented here. For implementation simplicity, direct parameter representation is removed. Instead, accumulator array counters correspond to pixel coordinates, and collect evidence for oriented lines passing through their specific spatial position.

The finite length voting process still results in slightly impaired line localization. To address this problem, we introduce a filtering process which ensures that completed line segments have support on both sides of a gap. This provides a mechanism for removing small spurious lines as well as trimming existing line segments, allowing robust filling-in to be done without sacrificing line end localization.

The enhanced Hough transform model contains four steps: 1) *Edge Detection*: at a full spectrum of orientations and spatial scales. 2) *Transformation*: by allowing feature points to vote for the line segments passing through them. 3) *Line End Localization*: by filtering detected line segments. 4) *Recombination*: of line segments detected at each orientation and spatial scale. Implementation details of each are discussed below.

2.2.10.1 The Evidence Summation Neural Network

Previous work has shown how the Hough transform can be cast in a connectionist architecture [Sab85]. Pixel based feature properties (thresholded oriented edges) are represented in neuron-like node elements, which cooperatively pass information to similar node elements containing parameter space information. Nodes in the parameter space record a level of confidence (vote totals); totals above some threshold “fire” the neuron, indicating the presence of the parameterized object in the image. The image to parameter space mapping determines the pattern of

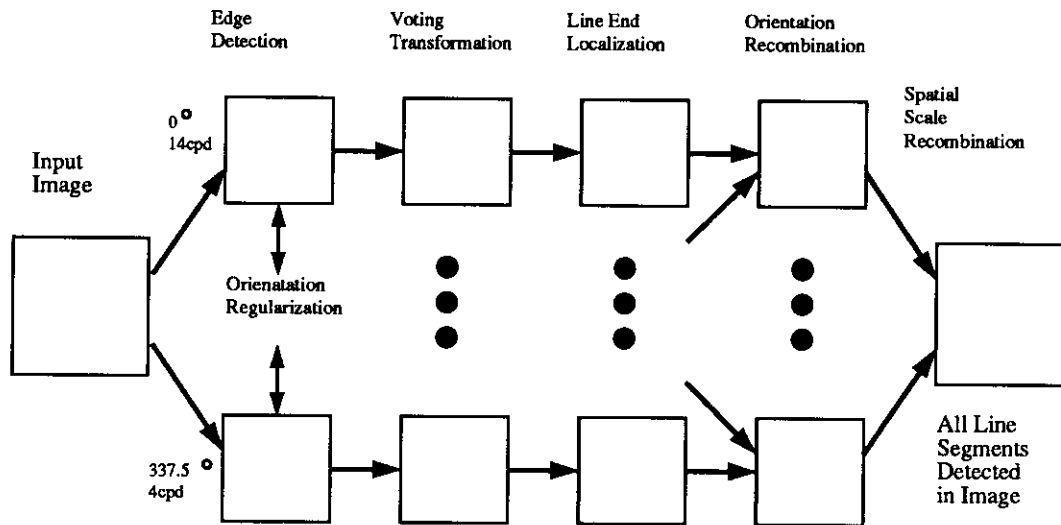


Figure 2.5: The enhanced Hough transform network. Edges are detected from the image, and then compete using a winner-take-all mechanism. Remaining points vote for lines passing through them using orientation and offset information. Evidence layers are recombined to yield all lines present in the image.

connections in the network.

Our final architecture is multi-layer feed-forward network (Fig. 2.5). An input image is filtered for oriented edges using a difference of offset Gaussian (DOOG) model [You91] at every 22.5° of orientation, and at four separate spatial scales (4, 8, 12 and 14 cycles per degree). Each orientation and spatial scale combination is processed with a separate layer of nodes, where each node in the layer has an identical connection pattern to encode the appropriate edge detection convolution. Within a spatial scale, orientations compete using a winner take all method; each pixel may signal an edge at one orientation only. Remaining edge points increment the confidence counter of nodes lying on an oriented line centered at the edge. The thresholded outputs of these nodes signal the presence of a line passing through the corresponding spatial position.

End points of the detected line segments are then localized using the line end filter described above. As with edge detection, the filter mask is encoded in the connection strengths of a layer of processing nodes. For a given spatial scale, all oriented line information is then combined by simply “and”ing information from the separate orientation layers. Spatial scales are combined by taking final line segments to be those which persist across two or more scales.

2.2.10.2 Hough Transform Simulation Results

The network is able to detect most real and illusory contours in simple input images. Lines corresponding to the outline of a figure completed despite gaps in the border are shown in Figure 2.6. The network was also able to fill-in illusory contours which were collinear with their inducing segments (Fig. 2.7). Here, normal contours as well as contours bounding the illusory bar were found.

The network also performed well with real world images (Fig. 2.8(a)). However, the network was unable to fill-in across gaps when they became too large. Increasing the size of the voting neighborhood expanded the gap size that could be crossed, but resulted in localization errors which could not be corrected through the line end filtering process. The network also had problems in disambiguating when to fill-in across a gap by completing lines which were not boundaries of surfaces, real or illusory. Varying the size of the local voting neighborhood across spatial scales might provide a method for addressing problems of this nature; our architecture transforms each scale separately, making this possible. A more intelligent (adaptive; uneven weightings of various cues) transformation and evidence collection scheme will prove to be a valuable tool for some perceptual completion tasks. However, this model of contour completion does not seem to be directly

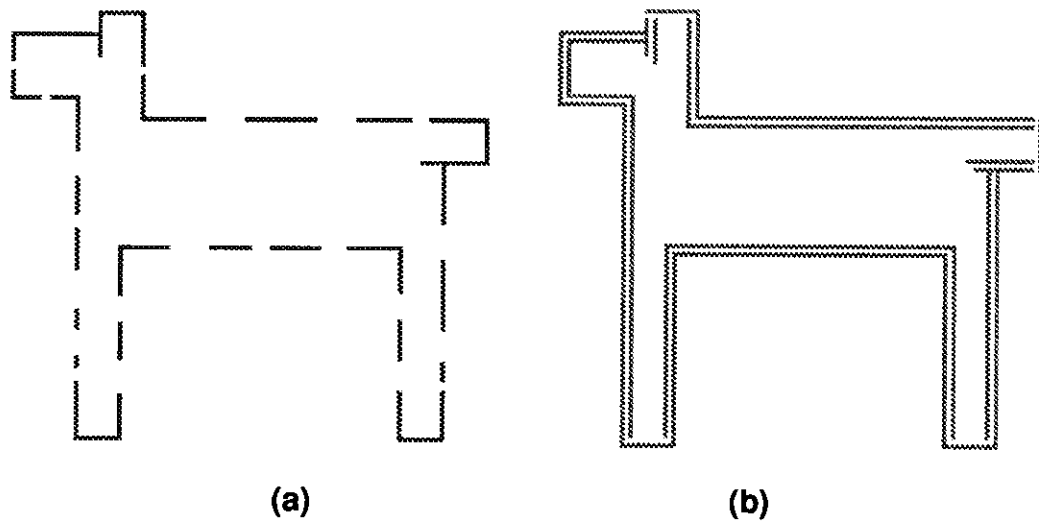


Figure 2.6: (a) An input image showing the broken outline of a figure. (b) The network was able to detect lines corresponding to the complete boundary of the figure despite gaps in the border.

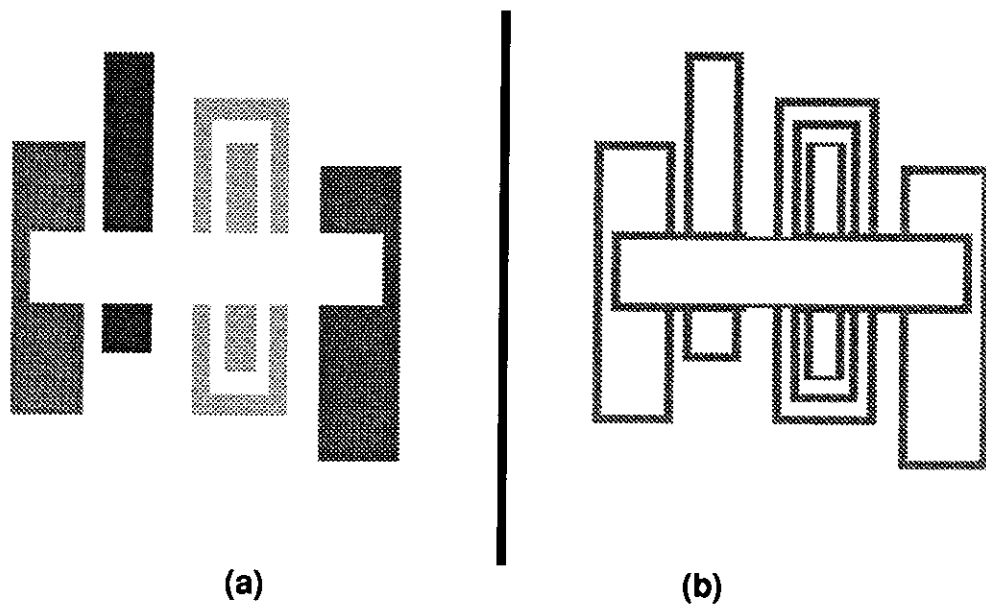


Figure 2.7: (a) An illusory bar can be seen occluding the broken rectangles. (b) Lines detected correspond to both normal contours and to the boundaries of the illusory surface.

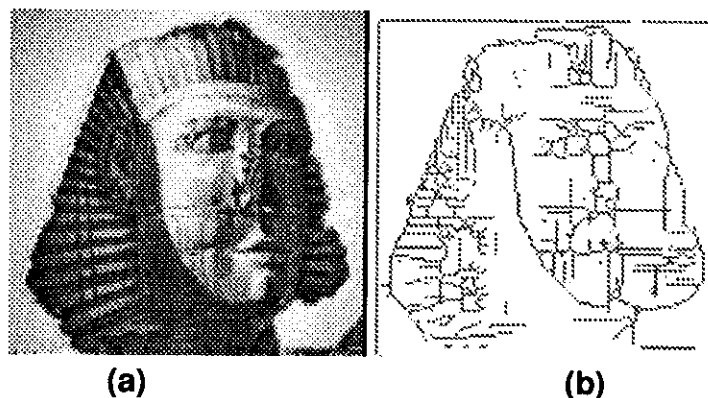


Figure 2.8: (a) A cluttered gray level image, and (b) The lines detected by the Hough transform network.

addressing the problem of illusory contour perception. The network is more likely to make amodal (occluded) rather than modal (occluding and illusory contour) completions [SN90]. In cases where the illusory contours are coincidental with the orientation of the inducing segments successful completion is achieved, but when the illusory contours are orthogonal (which is commonly the case), the occluded boundary is completed instead typically (Fig. 2.9).

2.3 General Contour Neurons

Although top-down and bottom-up theories both agree on the basic cause of illusory contour perception, the dividing issue is in where the mechanisms generating the perceptions are located. Much recent work has suggested that it is fairly common for the brain to exhibit so called intelligent behavior in lower

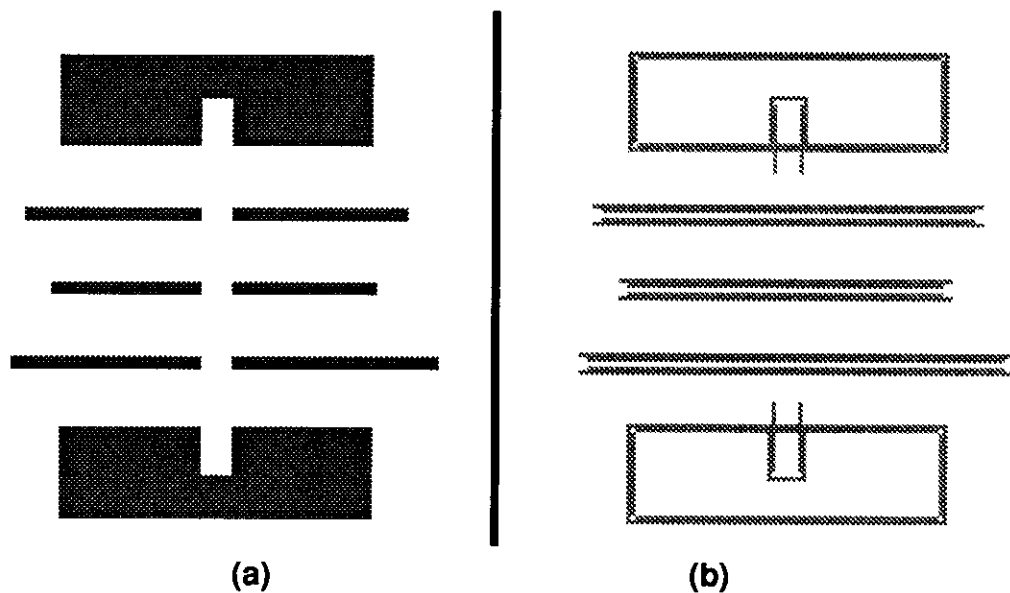


Figure 2.9: (a) An input image containing an illusory bar. (b) In cases where the illusory contour was orthogonal to the inducing segments the network had a tendency to make the amodal completions

level processes [Ram85b]. The tendency to attribute unexplained phenomena too quickly to cognitive black-box explanations without sufficiently exploring lower level rote mechanisms should be avoided. For illusory contours, this analysis seems to particularly pertinent.

Available data now seems to strongly support the idea of the human visual system beginning to extract occluding boundaries, and illusory contours at early layers of processing. The physiological findings of cellular responses in monkeys [HPB84] offer the most powerful support to this theory, with relevant data from psychophysics strengthening the case. The fact that illusory contours are subject to tilt after effects [PSN89], are insensitive to non-luminance defined cues [Pra85], and have an easily measurable maximum retinal extent [SG87] all point towards

a low-level visual function.

Discontinuous background structures, as typified by line terminations seem to be an absolute condition for the perception of illusory contours [SK90]. The correlation between line endings and occlusion has been noticed by many other workers [SSN89], and serves as the basis for many other models of illusory contour perception [PHB86, KWT87, McC90, MC91]. However, analysis and simulation results have showed that any model which relies solely on local discontinuity information for contour completion will produce spurious responses [SR92a, SR92b]. A simple illusory contour pattern helps to illuminate the cause for the failure of models such as these. Fig. 2.10 shows how two patterns with nearly identical line terminator information generate widely different illusory contour perceptions. A model based solely on line terminator information will produce nearly identical responses to both patterns.

Instead of merely linking line terminations, illusory contours define the boundaries of perceptual occluding surfaces [RG91]. The model proposed here uses the well documented interactions between depth and illusory contours [Cor72, GH74, NS90] to resolve this ambiguity, by exploiting the differences in depth between occluded versus occluding surfaces.

The model proposes the existence of binocular “General Contour Neurons” located in area V2 which are sensitive to occluding borders and can thus be driven by both real and illusory contours. Aligned sharp luminance discontinuities (line terminations) provide the driving stimuli to the illusory contour component of the neurons. The response of the neuron to these line terminations is modulated by excitation from depth sensitive cells signaling foreground surfaces, allowing the model to eliminate spurious completions. Furthermore, the model explains

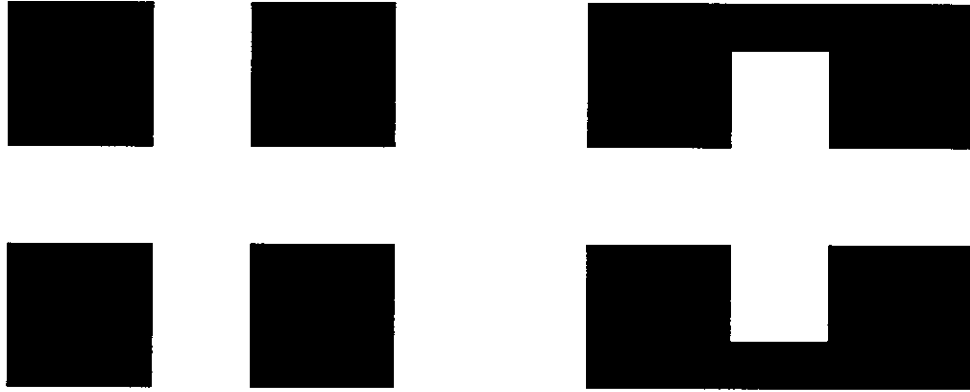


Figure 2.10: Minimal alteration of the image intensity profile in regions spatially separated from the “gaps” dramatically alters the saliency of the illusory contours perceived.

the three major perceptual effects associated with illusory contours: oriented contour perception, depth effects and increased brightness. A neural network implementation of the General Contour Neuron model is constructed and simulated, providing insights into the computational abilities of the model, as well as towards the type of information needed by an illusory contour detection mechanism. The network performs in correspondence with human psychophysical results for a broader set of illusory contour patterns than any available model.

CHAPTER 3

Computational Model

Our network consists of multiple layers of neuron-like nodes (cells), whose output is a positive real number correlated with average firing frequency [RHW85, SM91]. Temporal patterns of neuronal responses are not analyzed. Early layers of the network consist of computational models of simple, complex and hypercomplex cells which filter out “features” (edges, line terminations, etc.) to be aggregated at later stages. The desired cell property and sensitivity is controlled by the strength and topology of the connections within the cell’s receptive field. In effect, each cell in the layer performs an appropriate convolution with the “image” generated by previous layers to extract the desired “features”. No “learning” in the classical sense is performed by the network; the connections within the entire network are fixed, with two notable exceptions. The connections between cells composing the layer of “surface neurons” fluctuate in strength as a function of the input stimulus array to control activation spreading, and the connection strengths of the line terminator inputs to the General Contour Neurons vary as a function of the response of these surface neurons.

Illusory contours are signaled through layers of cells called General Contour Neurons proposed to exist in visual area V2. These neurons are an extension of the “contour neurons” proposed earlier [PHB86] which serve as the basis for the model described here. The GCNS are driven by two sets of striate inputs, one

sensitive to luminance edges, and the other sensitive to illusory contours. The latter input originates with proximal cells which are sensitive to contrast discontinuities represented by line endings. Responses from rows of perpendicularly oriented endstopped neurons are summed by interneurons over a spatial extent beyond the normal edge response. This summation is gated by similar activity on the opposite side of the elongated receptive field center. Discontinuity evidence is needed on both sides of a “gap” covered by the receptive field center in order to perform perceptual completion of an edge. Responses from this mechanism and from normal edge detectors are combined at the final General Contour Neuron, which is sensitive to both real and illusory contours (Fig. 3.1).

The response of the GCN to the line termination input is modulated by the activity profile of a layer of “surface neurons”. These neurons signal an abstract estimate of foreground surfaces present in an image by diffusively integrating information from elements which define visual surfaces: corners, line terminations and edges. Their functionality could be implemented by binocular neurons in early visual layers (V2), or by neurons in areas further along in the cortical hierarchy involved in form and depth perception (V5). Here, they represent a lumped sum model of simple surface depth processing. The simple feedforward explanation of illusory contours [PHB86] is expanded upon by adding: 1) explicit grouping of line terminations in a manner which yields relative depth information [HP87], 2) Detection of illusory curvature as well as straight segments to better define illusory surfaces, and 3) excitation from layers of “surface neurons” to modulate the GCN response to line terminations. An overview of the computational stages and information flow of the network is shown in Fig. 3.2. The three components (Feedforward, Recurrent and General Contour Neuron) are described in

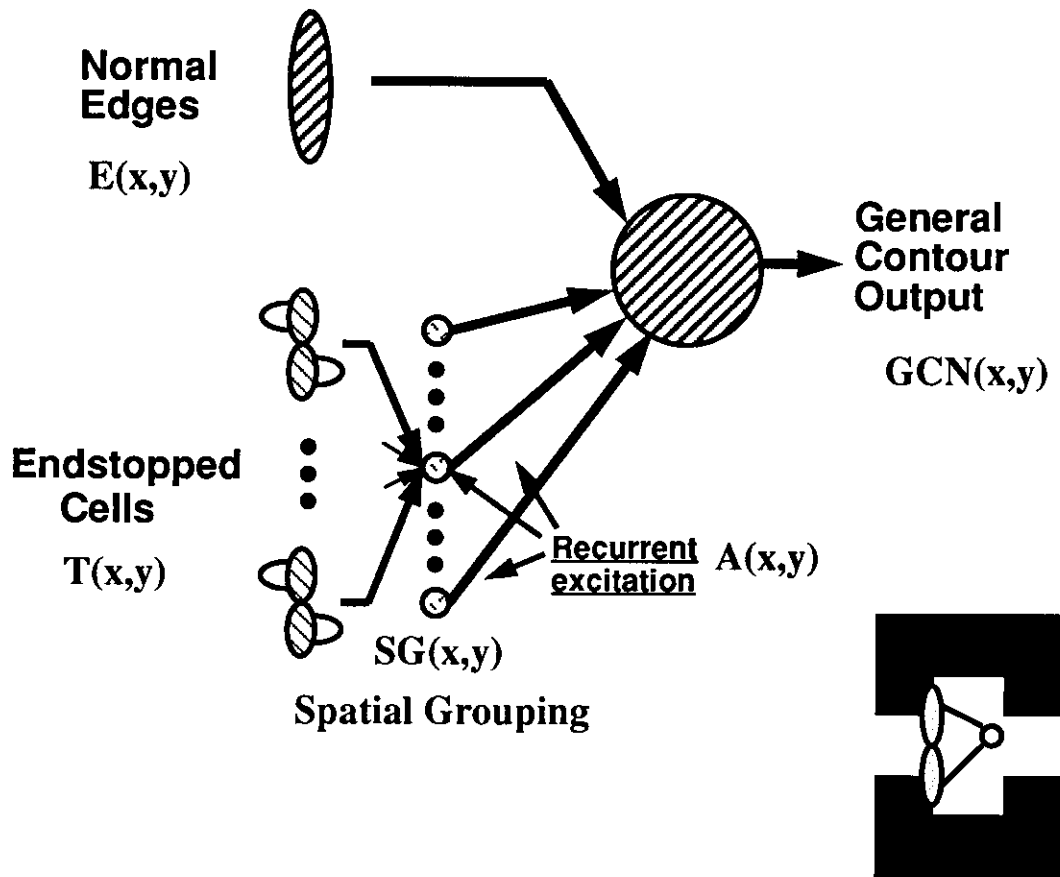


Figure 3.1: The General Contour Neuron. The cell receives input from two parallel sub-systems: luminance edges and illusory contours. The illusory contour component is driven by summation of orthogonally oriented endstopped cells. Recurrent excitation modulates the response of the cell to the grouping inputs.

detail below.

3.1 Feedforward Component

The feedforward component of the network contains layers of cells tuned to “features” to be aggregated by the General Contour Neurons. Our model of edge detection (simple cells) is a difference of offset Gaussian (DOOG) function [You86]. Layers of the network compute edge responses ($E(x, y, \theta)$) at different orientations (every 22.5°) by convolving DOOG filters with an image intensity profile $I(x, y)$:

$$E(x, y, \theta) = (G(x - x_o, y, \theta) - G(x + x_o, y, \theta)) \otimes I(x, y) \quad (3.1)$$

where:

$$G(x, y, \theta) = \frac{1}{2\pi\sigma_x\sigma_y} e^{-\left(\frac{(x'-x_o)^2}{2\sigma_x^2} + \frac{(y'-y_o)^2}{2\sigma_y^2}\right)} \quad (3.2)$$

is a standard oriented (orientation θ) two-dimensional Gaussian kernel centered at location (x, y) . σ_x and σ_y are the width of the Gaussian in the x and y directions respectively. (x_o, y_o) is the loci of the receptive field, and $(x', y') = (x\cos\theta + y\sin\theta, -x\sin\theta + y\cos\theta)$. Responses are half-wave rectified and passed through a sigmoidal non-linearity [SM91].

Line terminations ($T(x, y, \theta)$) are detected using a modification of a proposed hypercomplex cell model [DZC87] based on a difference of simple cell responses. The responses of two simple cells of the same orientation tuning but of different spatial extents are combined to yield endstopping inhibition. The larger spatial scale response is subtracted from the smaller one, resulting in a net receptive field with inhibitory end regions and side lobes. Our model incorporates a slight offset between the two receptive field centers to generate asymmetrical end-stopping

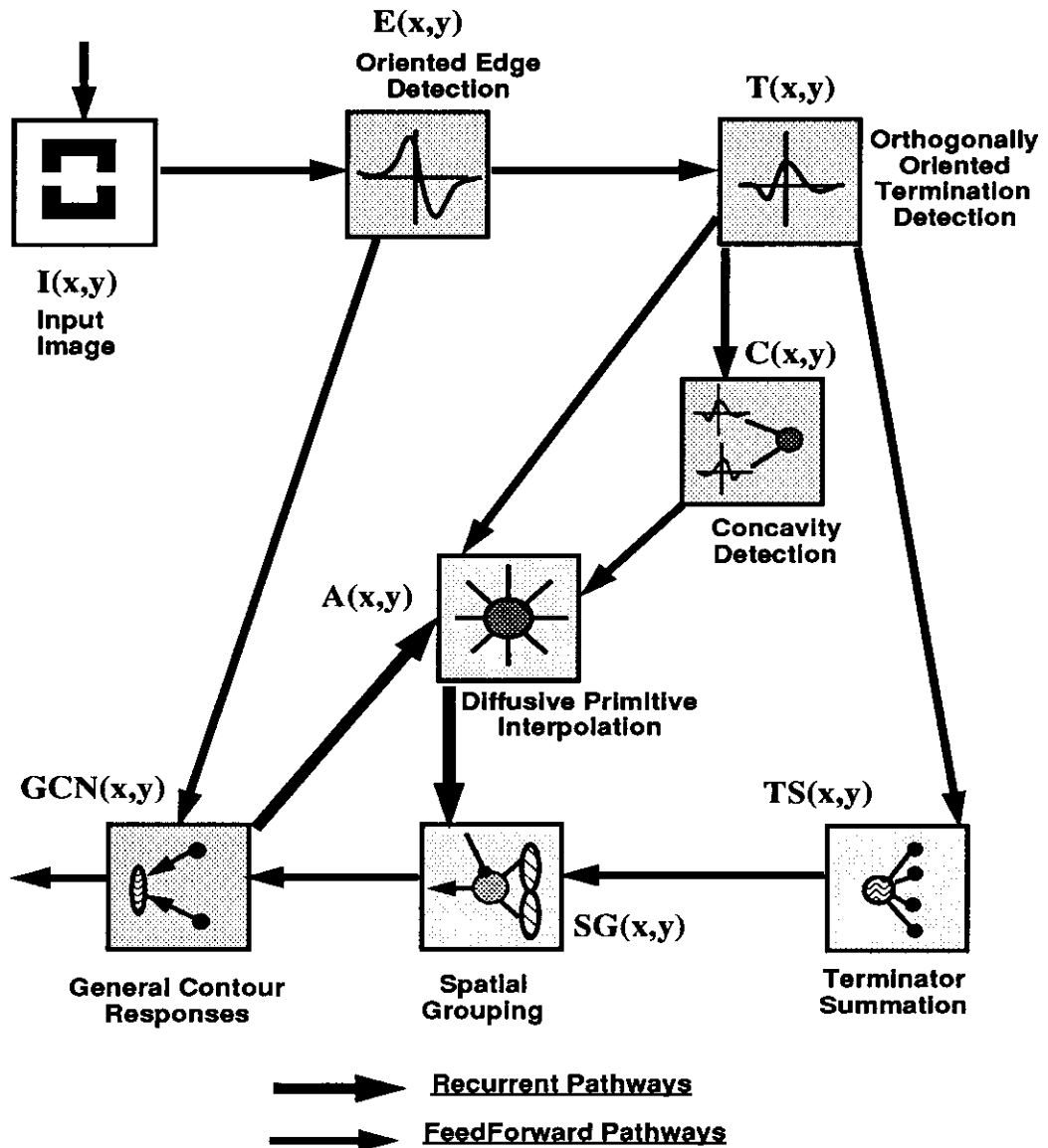


Figure 3.2: (a) The network architecture. Inputs to the General Contour Neurons are filtered by early layers of the network. Terminator outputs feed into a spatial grouping layer which pools for information on both sides of the gap. General Contour responses are a combination of edges, spatial grouping and recurrent excitation from surface activation levels.

inhibition. The resulting hypercomplex cell responds strongest to an oriented line ending. To help alleviate false responses from the hypercomplex cells [HRH92], the larger (inhibitory) cell response is weighted slightly larger ($\lambda_2 > \lambda_1$ in equation below). For a horizontal hypercomplex cell (simple cell receptive field centers offset along the x-axis),

$$T(x, y, \theta) = \lambda_1 E_i(x, y, \theta) - \lambda_2 E_j(x + x_o, y, \theta) \quad (3.3)$$

where λ_1 and λ_2 are response weighting constants, and E_i and E_j are different layers of simple cell responses as defined in equation 3.1. Responses are again half-wave rectified.

At each spatial position, feature responses are normalized by those of similar features at all other orientations (ie. edges compete with other edge responses across all orientations) [Hee90]. For a given feature at orientation θ and position (x, y) , the response $R(x, y, \theta)$ is given by:

$$R(x, y, \theta) = \frac{R_1 R(x, y, \theta)^2}{\Phi + \sum_{\alpha \in \Theta} R(x, y, \alpha)^2} \quad (3.4)$$

where Φ is a saturation constant, R_1 keeps the responses within the desired range (here 0 - 255), and α sums over orientations. This introduces a degree of contrast independence as well as response stabilization into the network; otherwise for example, a 22° line terminator with high contrast may give a higher response at 45° than an actual 45° degree line ending with low contrast.

Edges and line terminations compose the feature set required to drive the feedforward component of the network. Line terminations provide the primary input to the illusory part of the General Contour Neurons; no illusory contours can be completed without this input [SK90]. These terminations are grouped to yield information about the relative position of the occluding illusory surface.

Illusory surfaces usually overlay a discontinuous background structure; knowing the direction of the line terminations (from hypercomplex cells with asymmetrical end inhibition) provides foreground/background data. Each GCN is tuned to an illusory contour explicitly bounding an illusory surface. For example, in the case of a vertical illusory contour, there are two “vertical” GCNs, one signaling the edge of an illusory surface occluding “from the left”, and one “from the right”. A GCN signaling an occlusion “from the right” would require line terminations abutting the illusory edge from the left (see Fig. 3.3).

To produce a response, a GCN requires evidence about line terminators on each side of the receptive field center, corresponding to evidence on both sides of a perceptual gap. The effective GCN receptive field is bimodal; responses on each side of the receptive field center are summed separately, but responses from both sides (defined as response summations above some threshold Ψ) are necessary to fire the GCN. In the immediate region of the GCN, only line terminations of the preferred occlusion direction of the GCN are summed (from hypercomplex cells with the proper endstopping profile). If this evidence is present on both sides of the gap, then the total terminator summation can be possibly supplemented by line terminators of the opposite direction, summed across a slightly larger region (more distal image features such as corners cannot induce an illusory contour, but can increase the perceptual strength of an existing illusory contour). Determining the neighborhood size over which to integrate terminator information was an open parameter in the model; we used values between 0.5 and 2.0 visual degrees, in correspondence with psychophysical measurements of the maximum size gap which can be perceptually crossed by an illusory contour [SG87]. For a horizontal

GCN (summation occurring along the x-axis),

$$\begin{aligned}
 TS(x, y, \theta) = & \left(\left(\sum_{x=x-\delta}^{x, y_1} T(x, y, \theta) - \Upsilon \right) \&\& \right. \\
 & \left. \left(\sum_{x=x}^{x+\delta, y_1} T(x, y, \theta) - \Upsilon \right) \right. \\
 & \left. \mp \left(\sum_{x=x-\delta}^{x+\delta, y_2} T(x, y, \theta + 180) \right) \right) \quad (3.5)
 \end{aligned}$$

where $TS(x, y, \theta)$ is total terminator evidence summation at position (x, y) and orientation θ . $T(x, y, \theta)$ is line termination responses as per equation 3.3, and $\&\&$ represents a gating mechanism requiring responses on both sides of the receptive field center. If the first component (from $T(x, y, \theta)$) is > 0 , the second component (from $T(x, y, \theta + 180)$) is added to the response (\mp represents a conditional addition). The width of the grouping is fairly small, usually equivalent to 2 or 3 pixels, producing a thin, oriented GCN receptive field.

In addition to GCNs tuned to straight illusory contours as described above, our model includes a mechanism for the detection of illusory concavities (corners). This is in accordance with the ability to perceive illusory corners in displays such as the Ehrenstein illusion [Ehr41]. Here, the sections of the bimodal receptive field of GCN are oriented orthogonal to each other (resulting in an “L” shaped construct). Specific hypercomplex cell responses are once again summed to yield the relative position of the occluding surface bounded by the illusory corner. Our model currently includes GCNs detecting straight contours at 16 different orientations (every 22.5°), and at right angle corners. The model can easily be extended to detect illusory segments of any arbitrary degree of curvature.

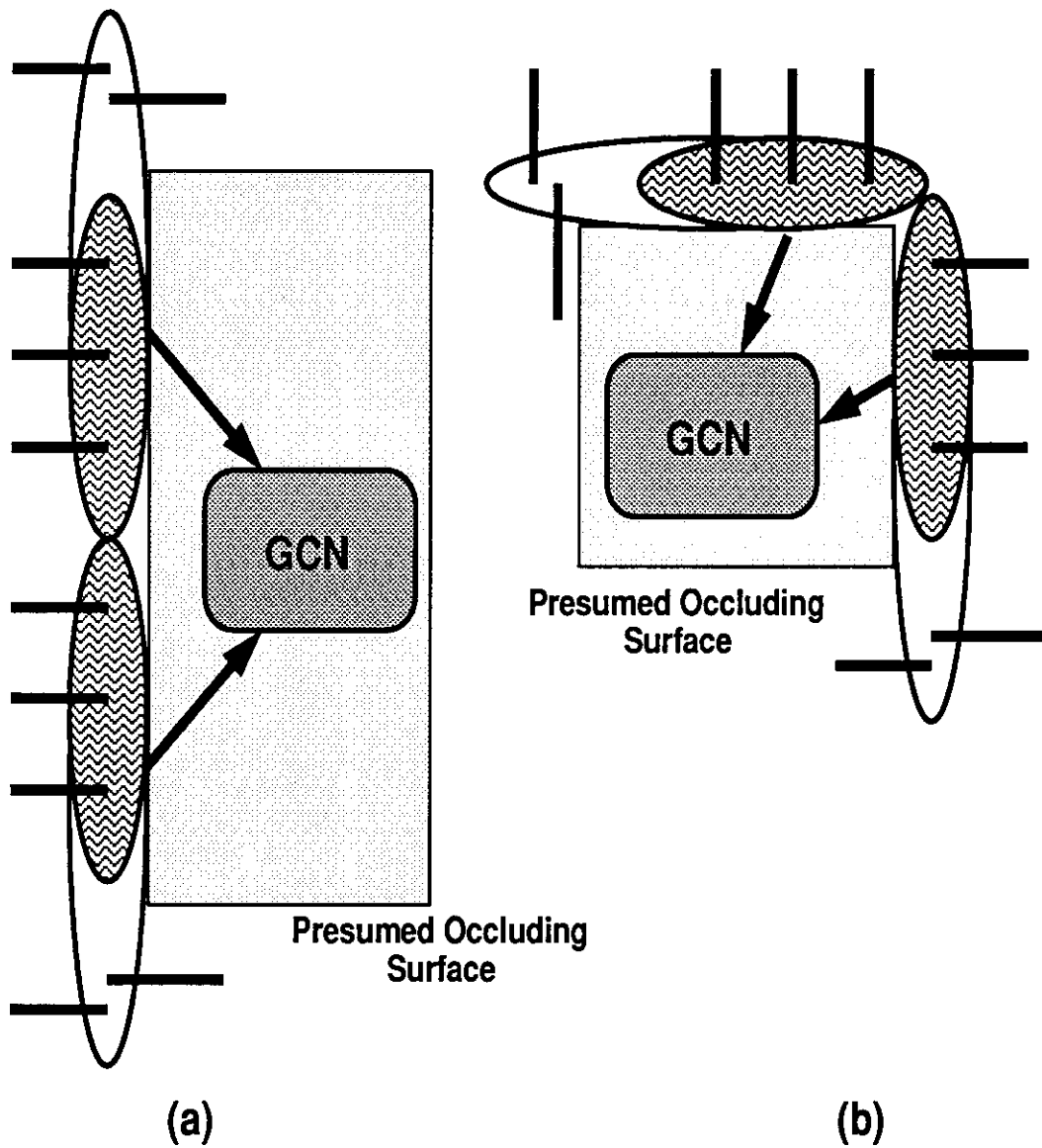


Figure 3.3: The receptive field profile of line termination groupings for (a) a GCN detecting a straight illusory contour, and (b) a GCN tuned to the detection of a right angle corner. Each pools asymmetrical hypercomplex cell responses consistent with the relative position of the occluding surface.

3.2 Recurrent Component

The second component controlling the activities of the GCNs is recurrent excitation, which facilitates the GCN's response to hypercomplex cells, enabling contour completion. Illusory contours bound perceptual surfaces; thus the recurrent excitation component is derived from estimates about visual surfaces present in a scene, signaled by layers of surface neurons. Utilizing the foreground/background interpretation of line termination grouping allows surface levels to provide confirming or contradictory evidence of a true surface boundary.

The visual surface estimate is generated by allowing contour features which best seem to define foreground surfaces (concavities, terminations and contours), to interact using a simple diffusive spreading activation mechanism [SHH87]. These features serve as a source of constant input and are thus the major determinant of surface neuron responses. Contour points with high curvature (corners) seem to be the most salient in capturing closed surface information [Att54], and in our model they represent the strongest "sources" of the diffusion. The corners ($C(x, y)$) are extracted by layers of cells which detect overlapping responses from orthogonally oriented hypercomplex cells.

$$C(x, y) = (T(x, y, \theta) - \Phi_2) \ \&\& \ (T(x, y, \theta + 90) - \Phi_2) \quad (3.6)$$

where $T(x, y)$ is defined in equation 3.3. Once again, both hypercomplex cells must respond (be activated at a level above some threshold Φ_2) at the same spatial location to drive the corner detection neuron.

Hypercomplex cell responses ($T(x, y, \theta)$) are obtained as part of the feedforward mechanism, and also serve as sources of the diffusion process. The final

source of diffusion is contours, as encoded by GCN outputs; the weighted combination of the summation across all planes of these three features serves as the time-dependent source ($S_t(x, y)$) of the system.

$$S_t(x, y) = \kappa_1 \sum GCN_t(x, y, \theta) + \kappa_2 \sum T(x, y, \theta) + \kappa_3 \sum C(x, y) \quad (3.7)$$

The k_i represent the relative contributions of the three components to the steady state source; values used were $\kappa_1 = 0.1$, $\kappa_2 = 0.2$, and $\kappa_3 = 0.4$. As the GCN responses are themselves dependent on the surface neuron responses, the recurrent excitation mechanism of the network is an iterative, dynamic subsystem. An analogy can be drawn to an integrated surface and edge based segmentation scheme.

Activation spreads from salient points $S_t(x, y)$ through the layer of surface neurons. Each surface neuron feeds activity to its neighbors according to a simple diffusion equation [SHH87]. The level of activity at each time step is used to determine the recurrent excitation fed to the GCNs. Thus, the GCN response evolves in time as the surface neuron activity profile settles into a steady state.

Anatomically, the outlines of such a scheme seem to be plausible. The primate visual cortex contains extensive feedback connections from higher visual areas (for example, V5) which modulate the responses of cells in area V2 to stimuli within their receptive field [LH88]. Conceivably, these connections carry more “global” information about a scene which could restrict the way early feature responses are processed. This “global” information may result from lateral interactions between cortical cells mediated by long distance intracortical connections [Gil88].

Given a set of variable strength sources $S_t(x, y)$ across an image, the activity level ($A_{t+1}(x, y)$) of a cell at position (x, y) and time $t + 1$ is modeled by the

following equation:

$$A_{t+1}(x, y) = (1 - \rho)A_t(x, y) + 1/n \sum_{i,j} \psi(i, j)[A_t(x, y) - A_t(i, j)] + \gamma S_t(x, y) \quad (3.8)$$

where: ρ is the decay rate (a positive number between 0 and 1), n is the number of neighbors of the cell (x, y) , $\psi(x, y)$ controls the strength of lateral connection and γ is a positive constant roughly equivalent to the decay rate. The term $[A_t(x, y) - A_t(i, j)]$ evaluates to 0 if $A_t(i, j) > A_t(x, y)$. $\psi(x, y)$ is a function of the strength of all computed contour response ($\sum_{\Theta} GCN(x, y, \theta)$) at the cell position:

$$\psi(x, y) = \frac{1}{N + \sum_{\Theta} GCN(x, y, \theta)}, \quad (3.9)$$

where N is a positive constant.

Contour responses ($\sum GCN(x, y, \theta)$) decrease the interaction between neighboring cells, providing a graded shunting of the diffusion process [GT88]. Cells contributing to the activity level via the summation are those in an eight connected neighborhood ($n = 8$) (see Fig. 3.4). Our simulations usually converged in 20-30 iterations, depending on the spatial separation between features. The precise interaction between surface activity levels ($A_t(x, y)$) and GCN responses is described in the next section.

3.3 General Contour Neuron

The main driving input to the GCN is the feedforward component represented by the summation of line-terminators ($TS(x, y, \theta)$). The GCN's response to this input is modulated by feedback from surface neurons ($A_t(x, y)$). Facilitation is provided when the $A_t(x, y)$ response is high at the border of the illusory surface signaled by a GCN. The relative level of surface neuron activities ($AG_t(x, y, \theta)$)

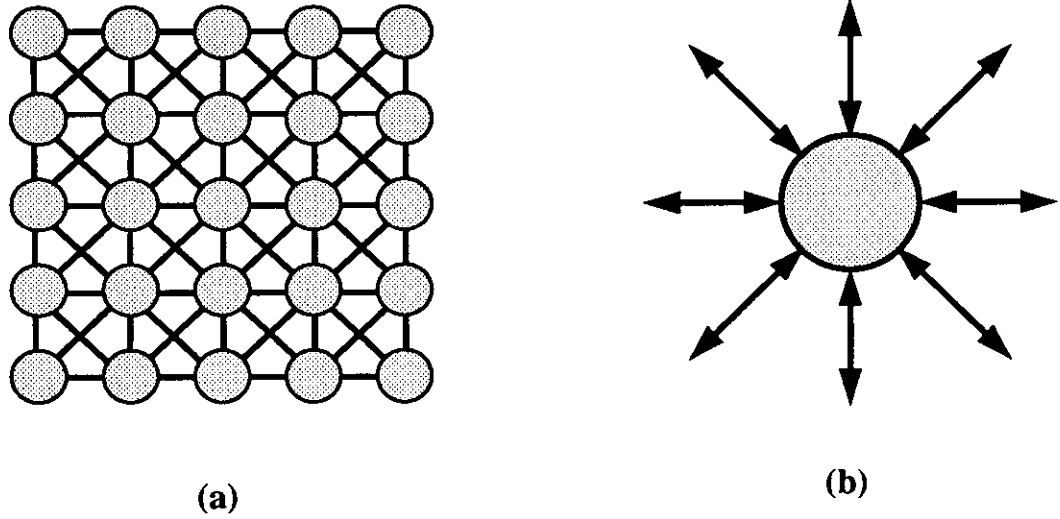


Figure 3.4: The diffusion process. Activity levels are communicated through connections between cells across the layer. Each cell connects to its 8 immediate neighbors. Activation levels spread through the cellular network until a steady state is achieved.

is determined by an interneuron which performs an oriented gradient detection (using the DOOG model) to determine the surface neuron activity gradient near the GCN.

$$AG_t(x, y, \theta) = (G(x - x_o, y, \theta) - G(x + x_o, y, \theta)) \otimes A_t(x, y) \quad (3.10)$$

The surface activity gradient must be compatible with the implicit depth gradient of the illusory contour signaled by the GCN. The absence of this gradient (or if it contradicts the depth preference of the GCN) reduces or removes the recurrent excitation, making the GCN less responsive to its hypercomplex cell inputs.

The spatial grouping ($SG(x, y, \theta)$) or illusory contour component of the Gen-

eral Contour Neuron is a non-linear function of the strength of the termination responses lying within its receptive field. This function is modulated by the activity of the surface neurons by shifting the response profile curve. Where the surface gradient is strong, it is possible for only limited terminator responses to fire the cell; where it is weak or absent, very strong terminator responses are required to produce a response.

$$SG_t(x, y, \theta) = K \frac{1 - e^{\frac{\Gamma_t(x, y, \theta) - TS(x, y, \theta)}{\tau}}}{1 + e^{\frac{\Gamma_t(x, y, \theta) - TS(x, y, \theta)}{\tau}}}, \quad (3.11)$$

where

$$\Gamma_t(x, y, \theta) = M e^{-mAG_t(x, y, \theta)} \quad (3.12)$$

$\Gamma_t(x, y, \theta)$ is an inverse exponential of the surface activity gradient which allows proper shifting of the spatial grouping response profile function. K, M, m and τ are positive constants and fixed parameters of the model.

Edges and spatial groupings are computed at multiple orientations at every spatial position. These responses are combined at layers of General Contour Neurons, each of which signals all contours, real or illusory, detected at a specific orientation and spatial position. Accordingly, the combined response of the GCN is given by:

$$GCN_t(x, y, \theta) = E(x, y, \theta) + SG_t(x, y, \theta) \quad (3.13)$$

The network, with a labeling of each processing layer is shown in Fig. 3.2. An input image is filtered for oriented edges by layers of simple cells ($E(x, y, \theta)$). These edges serve as an input both to layers of hypercomplex cells ($T(x, y, \theta)$), and to the GCNs themselves. Hypercomplex responses are summed ($TS(x, y, \theta)$),

and grouped ($SG(x, y, \theta)$). The grouping is controlled by the activity gradient ($AG(x, y, \theta)$), obtained by performing a gradient detection on surface neuron activity levels ($A(x, y)$). These activity levels are determined by a diffusive interaction between salient image points ($T(x, y, \theta)$, $C(x, y)$ and $GCN(x, y, \theta)$). The integration of feedforward and recurrent components performed by the General Contour Neuron is shown in Fig. 3.1.

CHAPTER 4

Simulation Results

4.1 Methods

Simulations presented in this paper were performed using the UCLA-SFINX network simulator [MS92] running on an RS/6000 workstation. UCLA-SFINX allows the construction and simulation of large scale fixed or variable connection networks, with X-windows based graphics utilities for viewing simulation outputs. The functionality of the network is specified by C language source code which is linked in with the simulator core.

The network consists of multiple 128x128 unit layers, with each unit linked to a specific pixel location. Within each layer, all units had identical connection patterns to encode their receptive field profile. The network contained 32 layers of simple cells (16 orientations at 2 spatial scales), 16 layers of hypercomplex cells (both asymmetrical inhibition patterns for 8 orientations; contrast pairs of simple cells, those at 180° orientation offsets, were combined to yield contrast insensitivity), 16 layers of terminator summations (one summing across each layer of hypercomplex cells), 4 layers of corner detection cells, 1 layer of surface neurons, and 20 layers of General Contour Neurons (four corner detecting layers and one for each terminator summation layer). All told, the network contained roughly 1,400,000 units, and in upwards of 40,000,000 connections. Simulation times were

on the order of minutes, mostly spent performing convolutions to obtain simple cell responses.

Input patterns were presented as 128x128 pixel grey level (256 grey levels) images, representing an area of 16 square degrees of foveal vision. Patterns selected for testing were from three categories: 1) standard illusory contour images popular in the literature to test the basic computational abilities of the model, 2) illusory patterns which had proven difficult for existing models to process to test the flexibility and robustness of the model, and 3) “real-world” patterns to test the performance of the ability of the model to perform with normal images. The General Contour Neuron is a model of visual processing and should perform equally well with illusory contour and regular stimuli.

The parameter set used was identical for all simulations. Most parameter values were determined by the geometry and connection patterns desired in the network, however some, such as gain control thresholds, had their values determined after some experimentation. Once acceptable values were obtained, they were fixed for all experiments. The contrast normalization of the network proved useful here, allowing the parameters of the network to remain fixed despite alterations in the range of grey scales in the input stimuli. A listing of all parameters and their values is shown in Tables 4.1 and 4.2.

Simulation outputs are in the form of response profiles of layers of cells. Each cell’s firing rate was scaled to a value between 0 and 255, with no response (level 0) represented by white, and maximal response (255) as black. Outputs shown are SFINX renderings of actual network layer responses. Performance of the network was evaluated by comparing the results to human psychophysical responses.

Parameter	Equation	Value
σ_x, σ_y	3.2	3 : 1 aspect ratio
λ_1	3.3	1.0
λ_2	3.3	1.2
Φ	3.4	5000
R_1	3.4	$\frac{255}{\frac{255^2}{\Phi + 255^2}} = 274$
Υ	3.5	100
δ	3.5	2
y_1	3.5	0.8
y_2	3.5	1.2
Φ_2	3.6	30
k_1	3.7	0.1
k_2	3.7	0.2
k_3	3.7	0.4

Table 4.1: The parameters used in the network.

Parameter	Equation	Value
ρ	3.8	0.05
γ	3.8	0.05
n	3.8	8
N	3.9	1
K	3.11	255
τ	3.11	48
m	3.12	0.1
M	3.12	220

Table 4.2: Additional parameters used in the network.

4.2 Results

The network is able to detect all luminance based and illusory contours in a variety of well-known illusory contour patterns. Additionally, the network produced results which compare well with human psychophysics with more difficult stimuli, including those with potentially ambiguous completions. An example of the network's outputs when presented with a simple illusory bar stimuli is shown in Fig. 4.1. Hypercomplex cells respond at the corners of the broken rectangles; however, these responses are not by themselves enough to fire the General Contour Neurons and complete any illusory contours. Corners, line terminations and contours are aggregated to serve as the initial activity level of the surface neurons. After several iterations, this process provides sufficient confirming evidence to allow the beginning of contour completion on the boundaries of the illusory bar. When a steady state is achieved, the boundaries of both the real horizontal rectangles and the vertical illusory bar are signaled by layers of GCNs.

Note that if these line terminations alone were taken as sufficient evidence, several extraneous completions would be generated (Fig. 4.2). The recurrent excitation component allowed the network to avoid these completions. Contours C & D were not completed due to lack of any surface neuron activity gradient in their vicinity; the sparse line termination evidence by itself is not enough to fire the GCNs in this area. A surface activity gradient exists in the region of contours E & F, however this gradient contradicts the depth assignment given by the line termination groupings to complete these contours. The direction of the line terminations predicts an occluding surface at the center of the image; the activity gradient is in the opposite direction, thus no completion occurs. Another example is shown in Fig. 4.3. Here, the contours bounding a "Kanizsa" square

are completed when confirming evidence is received from the surface neurons.

The performance of the model for a variety of illusory and real stimuli is shown in Figures 4.4 - 4.10. For each, the input image is shown (a), the final steady-state surface neuron activity levels in (b), and (c) shows the resulting responses of all General Contour Neurons in the network. The network provides good completions of contours bounding illusory surfaces, while yielding surface neuron activity profiles which correspond well to the foreground surfaces perceived in the image.

Fig. 4.4 shows the result of the network when tested with an abutting grating stimuli. The surplus of hypercomplex cell responses reduces the dependence upon surface neurons, allowing the contour between the two halves of the grating to be detected. The potential contour completions around the borders of the grating were largely suppressed, something not achieved by models relying solely on local termination information [GM85, PHB86], but clearly evident in physiological experiments [HPB84, HP89, PH89]. Existing models of illusory contour detection are often unable to detect both the abutting grating border and the boundaries of a Kanizsa square without major modifications [MC91, McC90]; here both types are completed with an identical network.

The network was able to detect the borders of a horizontal illusory bar given by multiple inducers (Fig. 4.5). Here there are several possible completions which can be made between line terminations; the network made only those which are perceived by human observers. The network was also able to detect the boundaries of the Kanizsa triangle (Fig. 4.6). Although all terminations here do not lie orthogonal to the contours they induce, the hypercomplex cell responses were still strong enough to allow completion.

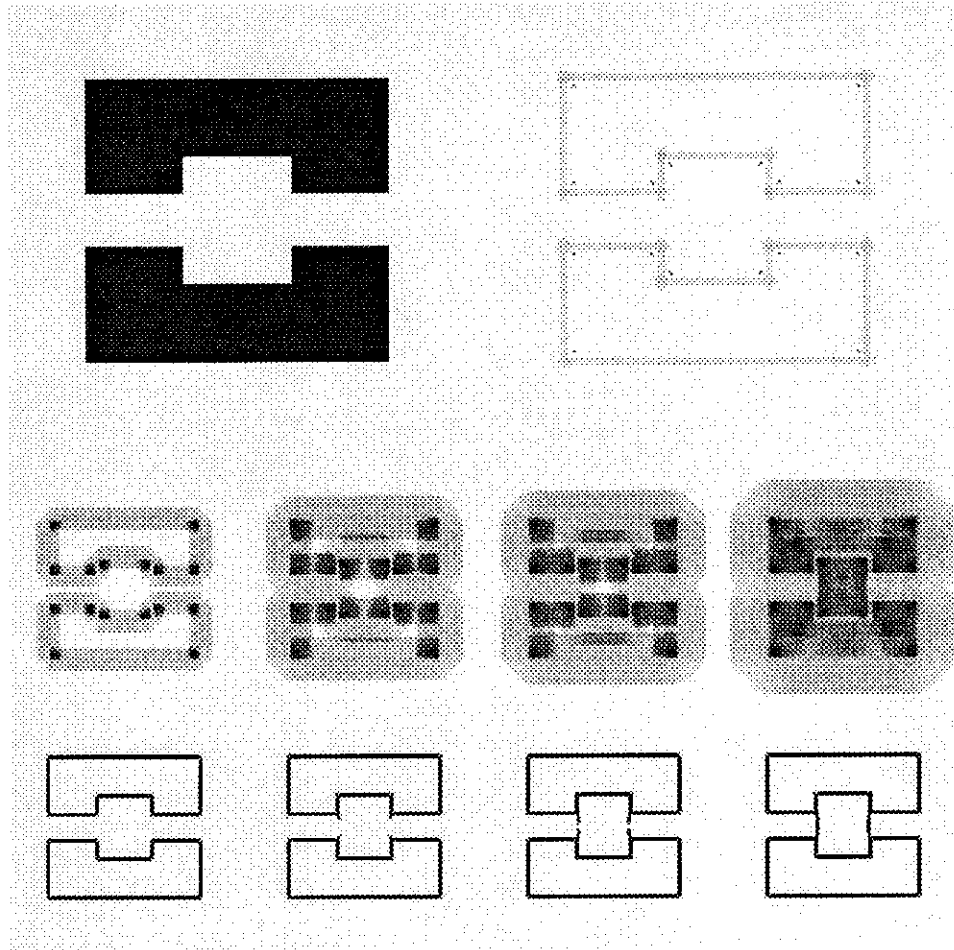


Figure 4.1: Simulation results of the network when presented with a simple illusory bar stimuli. (a) Shows the input image and the original diffusion sources. (b) Shows the time step output of the surface activation levels. (c) Shows the time step responses of all General Contour Neuron layers. Time steps shown are 0,10,20 and 30 iterations. As surface neuron activation levels spread, the GCNs begin to respond and signal the contour completion. At steady state, the boundaries of the illusory bar are clearly defined.

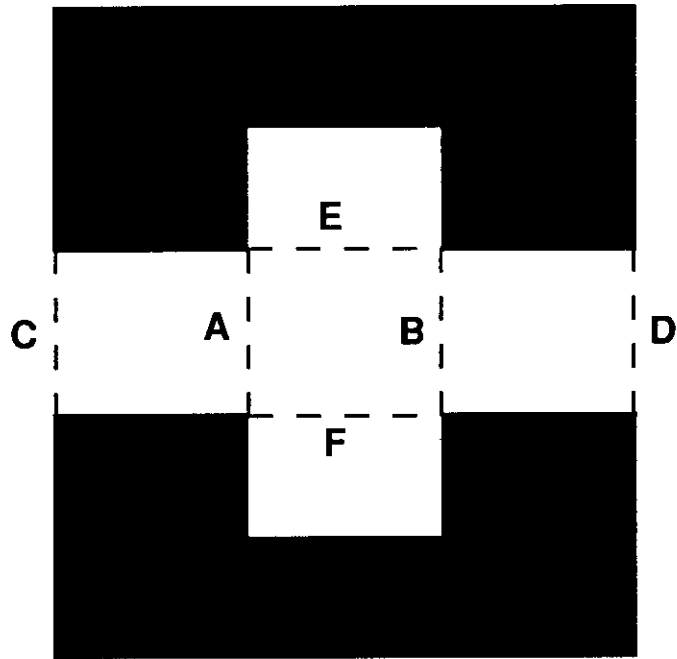


Figure 4.2: Possible contour completions based on line terminations with an illusory bar image. The General Contour Model makes only completions A & B, in correspondence with human psychophysics. Completions C, D, E & F are suppressed due to lack of recurrent excitation from surface neurons.

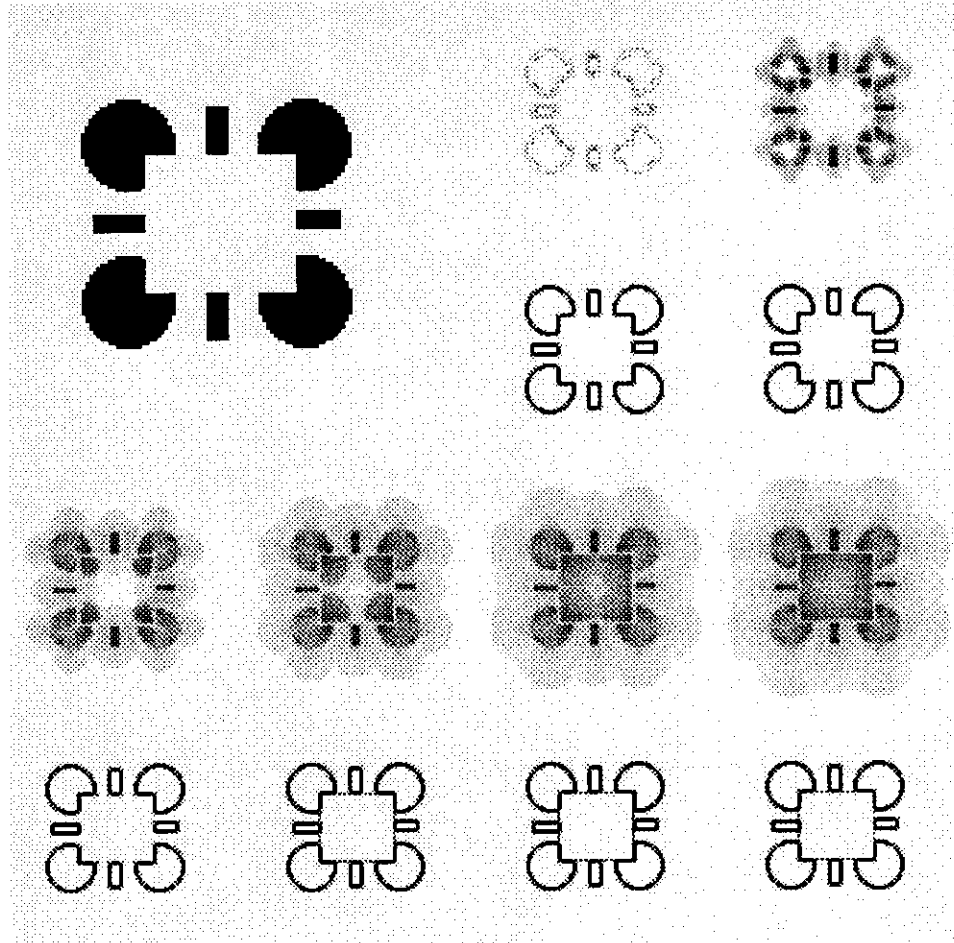


Figure 4.3: Simulation results of the network when presented with an illusory square stimuli. (a) The input image and initial sources. (b) The time step output of the surface activation levels. (c) The time step responses of all General Contour Neuron layers. Time steps shown are 10, 20, 25 and 30 iterations.

Illusory contours can be seen between inducers of opposite contrast polarity (see Fig. 1.2). The network was able to perform this type of completion because the hypercomplex cells were insensitive to contrast polarity, through the contrast independence of the hypercomplex cells (Fig. 4.7). Here also the contrast between the pattern and its background is sharply reduced, but the contrast normalization of the network performed well enough to allow the pattern to be processed properly.

The network was able to complete the boundaries of an illusory square drawn as a modification of the sun illusion [Ken78] (Fig. 4.8). The corners of the figure were signaled (although with slightly impaired localization) by GCNs tuned to illusory corners. Previous models have been unable to complete boundaries such as these because they impose the unrealistic requirement of the presence of line terminations from both directions [FE89].

Illusory contours are detected by the network through integration of cues which normally signal visual occlusion. When presented with a stimuli where the occluding boundary does have a luminance correlate, it is also detected by the General Contour Neurons through these same cues (Fig. 4.9). Finally, when presented with a “real-world” image, the network showed a limited ability to detect boundaries not marked by any continuous discontinuities (Fig. 4.10).

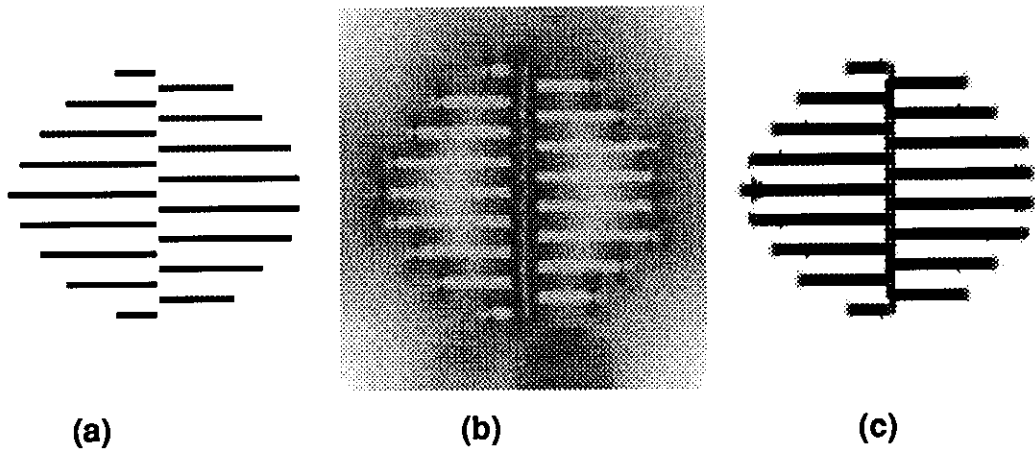


Figure 4.4: Simulation results. (a) Shows the input pattern presented to the network. (b) The final steady state surface neuron activity levels. (c) All contours detected by the network at steady state. The surplus of hypercomplex cell responses decreased the dependence upon surface neuron activity levels.

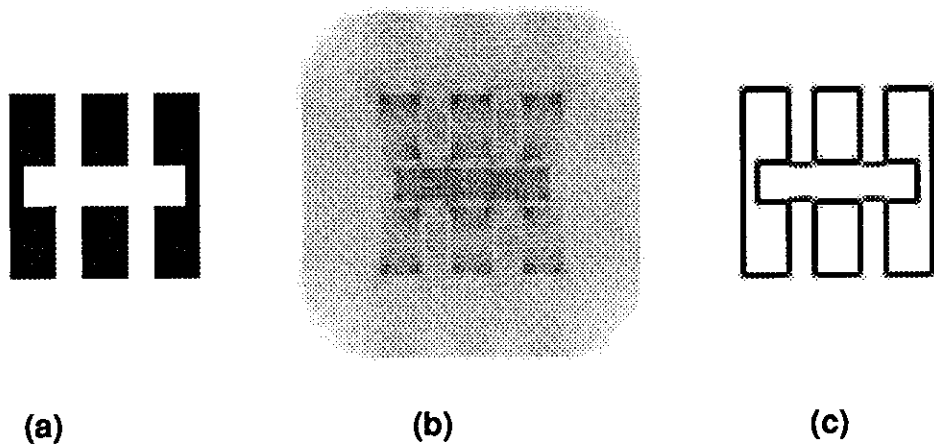


Figure 4.5: Simulation results. (a) - (c) as before. Of the many possible completions, the network made only those perceived by human observers.

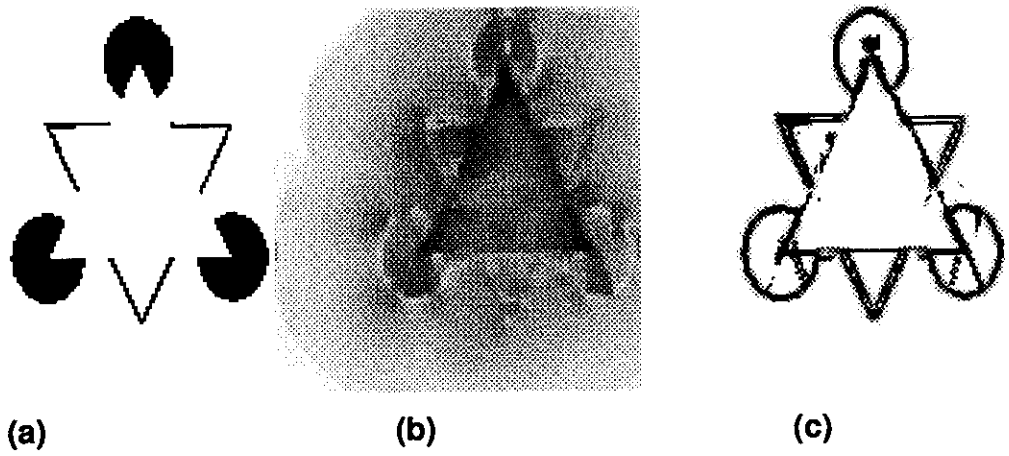


Figure 4.6: Simulation results. (a) - (c) as before. Although the line terminations were not orthogonal to the illusory contours, they were still detected by the network.

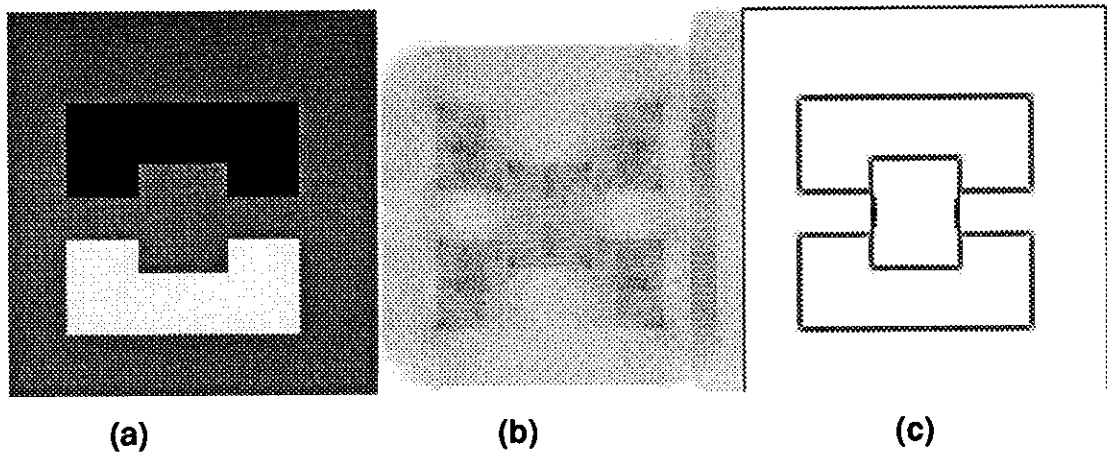


Figure 4.7: Simulation results. (a) - (c) as before. The contrast independence of the hypercomplex cell model allowed the network to complete between opposite contrast polarity inducers.

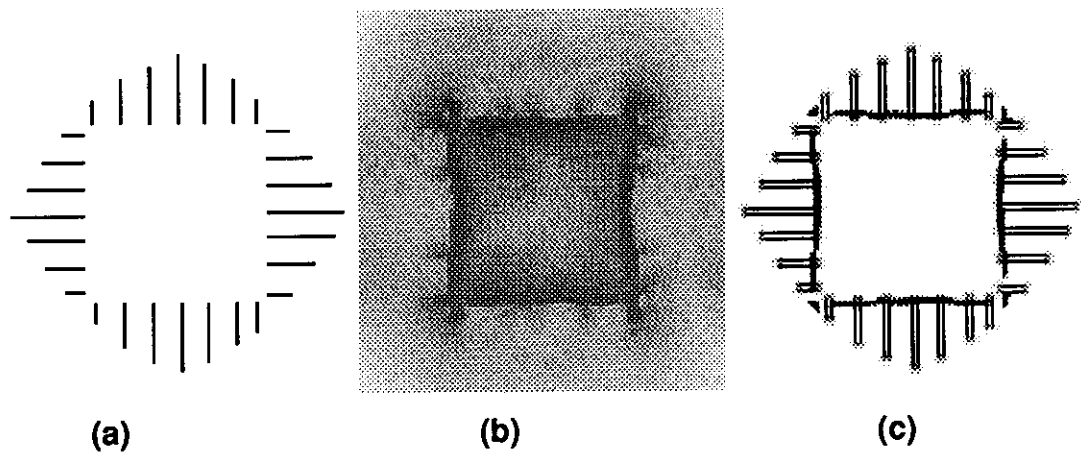


Figure 4.8: Simulation results. (a) - (c) as before. The corners of the square were detected by GCNs tuned to corner detection. The boundaries were completed despite the presence of line terminations from both directions.

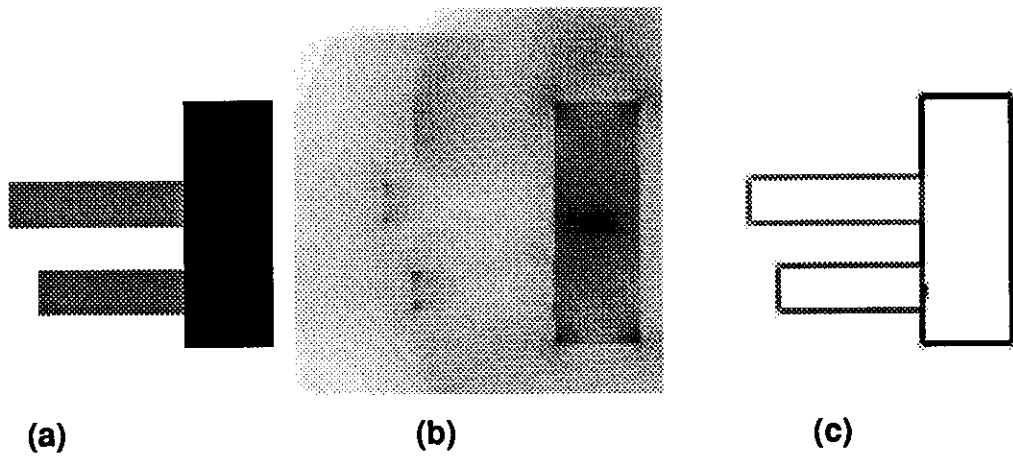


Figure 4.9: Simulation results. (a) - (c) as before. The occluding border was detected by the same mechanism used to detect illusory contours.

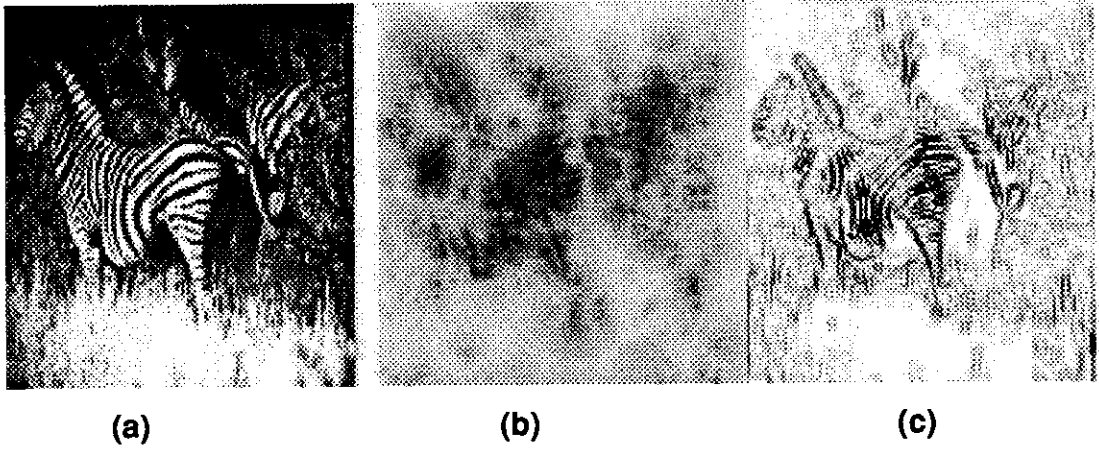


Figure 4.10: Simulation results. (a) - (c) as before. The network was able to partially detect the boundaries despite a lack of continuous discontinuities.

CHAPTER 5

Discussion

Recent studies of computer vision and computational modeling of biological vision systems have stressed the important role illusory contours may play in the visual segmentation process [Mar82, GM85, Ram87]. This thesis has attempted to quantify that role, by developing a framework addressing the need for illusory contours in the processing of images (ie. in the detection of occluding and discontinuity impaired surfaces), and by providing a computational model of illusory contour perception. The results presented here suggest that the apparently complex cognitive methods by which humans efficiently extract information from images can be explained through interactions of fairly simple neural networks operating on primitive features.

The computational models of illusory contour processing reported in the literature often perform properly for only a limited subset of illusory contour patterns [GM85, FE89], or are forced to radically adjust the functioning of the network to accommodate different types [McC90, MC91]. Our model's performance is comparable to human psychophysical results for a wide variety of illusory contour patterns, and is based directly on available physiological data. It can account for the three most notable perceptual effects observed in the illusory contour phenomenon: 1) Oriented contour perception, 2) Depth effects, 3) Increased brightness. Each is discussed below.

5.1 Oriented Contour Perception

Illusory contours have a very real perceptual feel, much like normal contours. The General Contour Neuron model predicts that some orientation sensitive cells in early visual layers (V2) which signal real contours also signal illusory contours [HPB84]. Higher visual processes which interpret the output of these cells would be unable to differentiate whether the response was due to an illusory or real contour, rendering the two types perceptually indiscriminable. Support for this comes from psychophysical data showing that illusory contours perform similarly to normal contours in a variety of visual tasks [PSN89, Ram85a, Ram86].

5.2 Depth Perception

Illusory surfaces often appear offset in depth from their background. The General Contour Neurons signal illusory contours as the border of an occluding surface, either illusory or real (Fig. 4.5, Fig. 4.9). Additionally, each GCN has an implicit depth gradient (which determines its dependence upon surface neuron activity levels). There is extensive psychophysical [Cor72, GH74, Jul71, NSS89, NS90, SN90] and physiological data [HPB84, PH89, HP89] to support the relationship between illusory contours and depth.

The model predicts that orientation sensitive binocular cells tuned to a disparity offset signal illusory contours as well as other types of depth boundaries. This could be directly tested by recording the responses of cells which respond to illusory contours to other types of depth boundaries, either stereoscopic or monocular. Recent modeling efforts have suggested that contrast polarity insensitive cells in early visual layers may be ideally suited to perform disparity

detection [ODF90]; the GCNs fit this hypothesis. Further, there is evidence that some depth boundaries can suppress illusory contour perception [GH74], and percepts similar to illusory contours can be generated by manipulation of depth cues without a luminance discontinuity correlate [Jul71, NS90].

5.3 Brightness Perception

Illusory surfaces are often marked by an unusual perception of brightness (or darkness) beyond those of physically identical background elements. Much recent work has focused on the possibility that what we perceive in visual surfaces is merely filled in from contrast (color or lightness) at the boundary [RG91, SG92]. Thus, having a contrast polarity sensitive illusory contour would yield a lighter (or darker) illusory surface, one whose brightness would appear all the more striking due the lack of actual contours separating it from its physically homogeneous background. Grouping of line terminations in a contrast polarity manner (ie. light terminators on black backgrounds) would allow computation of illusory contours with a luminance polarity [HP87]. Currently, our model combines contrasts of both polarities, allowing the completion of illusory contours between opposite luminance polarity inducers (Fig. 4.7). However, boundary detecting cells in V2 may be tuned for either contrast polarity or for foreground/background direction. Both types of grouping could be done; contrast pairs could be combined to yield relative disparity, and kept separate to allow brightness detection.

5.4 Anatomical Considerations

Anatomical and physiological data have shown that processing in the primate visual system is done through two functionally segregated pathways, the magnocellular and parvocellular [DE85, LH88, ZS88]. This separation begins in the retina and continues to higher visual layers, with limited pathway integration. The parvocellular pathway is mainly selective for form and color processing, while the magnocellular has been linked to the processing of depth, motion, and spatial relationships among objects [LH88]. Thus, illusory contours are likely processed in the magnocellular pathway. This is supported by psychophysical data; illusory contours cannot be perceived when the inducing elements vary from the background in only color. Because the magnocellular pathway is largely color blind, it would not be triggered by such a stimuli.

The General Contour model is based on physiological results showing responses of cells to illusory contours in area V2 [HPB84, HP89, PH89]. The GCNs could be located in the thick stripes of area V2 (see Fig. 5.1). Feedforward connections would come from from V1 simple cells and V1 or V2 high resolution (parvocellular) asymmetrical hypercomplex cells. Cells with this asymmetrical endstopping property have been reported in V2 by Peterhans et al. [PH91], and there is evidence for extensive interaction between the magno and parvocellular pathways in V2 [ZS88, EAF92].

General Contour Neurons receive recurrent excitation which modulates their processing of line terminator information. Cells in the thick stripes of V2 receive three major types of connections, feedforward from V1, recurrent from V2 thick and thin stripe regions, and feedback from higher visual layers, mainly V5 and possibly V4 [ZS88, EA90]. The recurrent excitation could be generated from

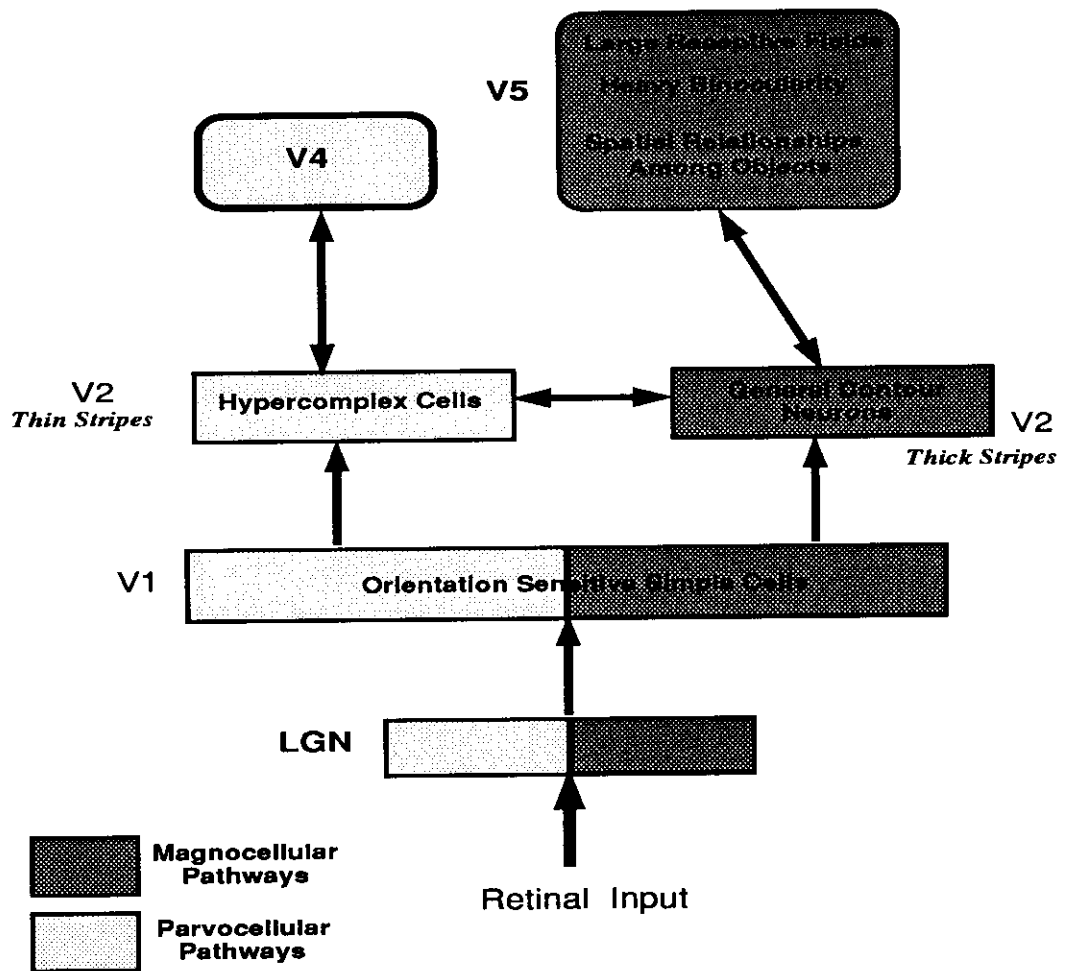


Figure 5.1: Speculative anatomical correlates of illusory contour processing by the primate visual system.

interactions between binocular neurons in area V2 which share data in order to represent continuous surfaces in depth [MP76]. There is evidence for lateral long-range connections between early visual cells which allow integration of information across the visual field [GW90]. Alternatively, the excitation could come through feedback from area V5, which has been implicated in depth and spatial relationship processing. The feedback connections from V5 to the magnocellular section of V2 are extensive; feedback connections outnumber feedforward connections in the primate visual cortex. Further, the manner in which feedback effects earlier processing seems to fit well with the role of recurrent excitation in the model: "...backward connections seem not to excite cells in lower areas, but instead influence the way they respond to stimuli within their smaller receptive fields." (from Zeki & Shipp, 1988). These feedback connections may serve additional purposes; because feedback typically draws from many diverse areas [DE85], it may represent the mechanism by which the various previously separated perceptual primitives are integrated [KK89]. This integration may explain the data showing interactions between illusory contours and other perceptual features [Ram85a, Ram86, RG91], or from "higher-level" variables such as memory [WS88] or perceptual set [CPT86].

The recurrent excitation of the GCN model allows suppression of some responses to aligned terminations which do not correspond to perceptual illusory contours. However, it could be that illusory contours and the spurious completions are both actually "seen" and signaled at V2, and that spurious completions are not perceptually suppressed until later in visual processing [Hey92]. Although this hypothesis cannot be ruled out without physiological experiments, it seems to stand in contrast to some organizational principles of the visual system. In-

creasingly, seemingly “cognitive” visual tasks are being proposed to be computed instead at early visual levels [Ram85b, NS92]. With the multitude of recurrent and feedback connections present, the information necessary to suppress these responses is available at V2. Performing suppression at lower levels would allow higher visual levels to focus computational processing on the surplus of intermediate level visual tasks which cannot be addressed at early visual levels.

5.5 Future Work

Although the General Contour Neuron model proved successful in the detection of illusory contours, several shortcomings exist which should be addressed in extensions to this work. Currently, line terminations are grouped at one receptive field size only ($y_2 = 1.4$ visual degrees in equation 3.5). Grouping at multiple scales, with possibly some interactions between the different scale groupings, would make the model more robust. Multiple scale processing is a technique the primate visual system has exploited to benefit other tasks [EAF92]. Multiple scale grouping of line segment evidence was used in the Hough transform model [RS91] to help the network cross gaps of different sizes, particularly with complex stimuli.

The contrast normalization of the network, although effective, does not represent a complete model of the interactions between early visual features [Hee90]. There is now evidence of extensive interactions between orientation sensitive cells in V1 [GW90, VDO89]. Implementation of interactions of these types would produce a better feature set for the GCNs, producing better results from operations on these features [Mes92], as well as allowing early layers of the network serve as a better model of area V1 processing.

The curvature and contrast detection used in the model is oversimplified and inadequate for complex, irregular stimuli. Currently, only right angle corners are detected, using overlapping hypercomplex cell responses (equation 3.6). Extending the mechanism of curvature detection to arbitrary curved elements is a necessity for processing of natural scenes, and essential for a model of visual contour processing. Several models for general curvature detection using hypercomplex cells exist [DZC87, WR89, VOL90], although none have been successfully implemented, or been proven to be biologically accurate.

The GCN model proposes that illusory contours bound closed surfaces, which are (at least partially) defined by corners and points of curvature. This assumption appears to be valid. However, there have been some recent reports of illusory contours being marginally perceptible in situations where they do not bound closed surfaces [PC92a]. These cases would limit the effectiveness of surface neuron activity levels to aid in the completion process. However, the mechanism through which line terminations are integrated still allows some contours to be completed in absence of surface information (Fig. 4.4). Additionally, not all closed surfaces are well defined by corner or curvature information, the major source of initial surface neuron activity levels. Here though, the ability of multiple types of image cues to define surfaces (such as line terminations) allows completion of the boundaries of surface without this curvature information (Fig. 4.8).

5.6 Conclusions

We feel that our model provides a reasonable interpretation of evidence about the visual processing of illusory contours. By using primitive estimates of foreground/background depth information (from surface neuron activity levels), our

model is able to successfully disambiguate potential illusory completions. A more realistic implementation of the lower layers of the network will help provide additional robustness. The model makes several predictions about organization of early layers of the primate visual system, and outlines a number of interesting experiments which would better address the computational mechanisms of this system. As more data becomes available about the visual processing of depth, the model can be expanded to make more concrete predictions, and to serve as a better model for occlusion detection in artificial vision systems.

REFERENCES

- [AK87] E.J. Van Allen and P.J. Kolodzy. "Application of a boundary contour neural network to illusions and infrared sensor imagery." In *Proceedings of the IJCNN*, San Diego, California, June 1987.
- [Att54] F. Attneave. "Some informational aspects of visual perception." *Psychological Review*, **61**(3):183–193, May 1954.
- [Bal81] D. H. Ballard. "Generalizing the Hough transform to detect arbitrary shapes." *Pattern Recognition*, **13**(2):111–122, 1981.
- [BBM88] Mary Bravo, Randolph Blake, and Sharon Morrison. "Cats see subjective contours." *Vision Research*, **28**(8):861–865, 1988.
- [BD75] Drake R. Bradley and Susan T. Dumais. "Ambiguous cognitive contours." *Nature*, **257**(5527):582–584, October 1975.
- [Cor72] Stanley Coren. "Subjective contours and apparent depth." *Psychological Review*, **79**(4):359–367, July 1972.
- [CPT86] Stanley Coren, Clare Porac, and Leonard H. Theodor. "The effects of perceptual set on the shape and apparent depth of subjective contours." *Perception & Psychophysics*, **39**(5):327–333, May 1986.
- [DE85] E.A. DeYoe and D.C. Van Essen. "Segregation of efferent connections and receptive fields in visual area V2 of the macaque." *Nature*, **317**:58–61, 1985.
- [DH72] Richard O. Duda and Peter E. Hart. "Use of the Hough transformation to detect lines and curves in pictures." *Communications of the ACM*, **15**(1):11–15, 1972.
- [DK83] R. H. Day and R. T. Kasperczyk. "Amodal completion as a basis for illusory contours." *Perception & Psychophysics*, **33**(4):355–364, April 1983.
- [DLB90] Birgitta Dresch, Jean Lorenceau, and Claude Bonet. "Apparent brightness enhancement in the Kanizsa square with and without illusory contour formation." *Perception*, **19**:483–489, 1990.
- [DZC87] Allan Dobbins, Steven W. Zucker, and Max S. Cynader. "Endstopped neurons in the visual cortex as a substrate for calculating curvature." *Nature*, **329**(6138):438–441, October 1987.

- [EA90] David C. Van Essen and Charles H. Anderson. "Information processing strategies and pathways in the primate retina and visual cortex." In Steven F. Zometzer, Joel L. Davis, and Clifford Lau, editors, *An Introduction to Neural and Electronic Networks*, pp. 43–72. Academic Press, New York, 1990.
- [EAF92] David C. Van Essen, Charles H. Anderson, and Daniel J. Felleman. "Information processing in the primate visual system: An integrated systems perspective." *Science*, **255**:419–423, January 1992.
- [Ehr41] W. Ehrenstein. "Über Abwandlungen der L. Hermannschen Helligkeitsscheinung." *Zeitschrift für Psychologie*, **150**:83–91, 1941.
- [FC75] J. P. Frisby and J. L. Clatworthy. "Illusory contours: Curious cases of simultaneous brightness contrast?" *Perception*, **4**:349–357, 1975.
- [FE89] Leif H. Finkel and Gerald M. Edelman. "Integration of distributed cortical systems by reentry: A computer simulation of interactive functionally segregated visual areas." *Journal of Neuroscience*, **9**(9):3188–3208, 1989.
- [GH74] R.L. Gregory and J.P. Harris. "Illusory contours and stereo depth." *Perception & Psychophysics*, **15**(3):411–416, June 1974.
- [Gil88] C.D. Gilbert. "Neuronal and synaptic organization in the cortex." In *Neurobiology of the Neocortex*, pp. 219–241, New York, 1988. Wiley.
- [Gin75] A. P. Ginsburg. "Is the illusory triangle physical or imaginary?" *Nature*, **257**:215–220, 1975.
- [GM85] Stephen Grossberg and Ennio Mingolla. "Neural Dynamics of Form Perception: Boundary Completion, Illusory Figures, and Neon Color Spreading." *Psychological Review*, **92**(2):173–211, April 1985.
- [GT88] S. Grossberg and D. Todorovic. "Neural Dynamics of 1-D and 2-D Brightness Perception: A Unified Model of Classical and Recent Phenomena." *Perception & Psychophysics*, **43**:241–277, 1988.
- [GW90] C. D. Gilbert and T. N. Wiesel. "The Influence of Contextual Stimuli on the Orientation Selectivity of Cells in Primary Visual Cortex of the Cat." *Vision Research*, **30**(11):1689–1701, 1990.

- [Hee90] David J. Heeger. “Nonlinear model of neural responses in cat visual cortex.” In *Computational models of visual processing*. MIT Press, 1990.
- [Hey92] R. von der Heydt. “Visual cortical mechanisms in figure-ground segregation.” Research Talk at Caltech, September 1992.
- [Hor86] B. K. P. Horn. *Robot Vision*. MIT Press, Cambridge, Mass., 1986.
- [Hou62] P. V. C. Hough. “Methods and Means for Recognizing Complex Patterns.” Technical Report U. S. Patent 3069654, 1962.
- [HP87] R. von der Heydt and E. Peterhans. “Ehrenstein and Zollner Illusions in a neuronal theory of contour processing.” pp. 729–734, August 1987.
- [HP89] R. von der Heydt and E. Peterhans. “Mechanisms of contour perception in monkey visual cortex. I. Lines of pattern discontinuity.” *The Journal of Neuroscience*, **9**(5):1731–1748, May 1989.
- [HPB84] R. von der Heydt, E. Peterhans, and G. Baumgartner. “Illusory contours and cortical neuron responses.” *Science*, **224**(4645):1260–1262, June 1984.
- [HRH92] Friedrich Heitger, Lukas Rosenthaler, Rudiger von der Heydt, Esther Peterhans, and Olaf Kubler. “Simulation of Neural Contour Mechanisms: from Simple to End-stopped Cells.” *Vision Research*, **32**(5):963–981, 1992.
- [IK88] J. Illingworth and J. Kittler. “A survey of the Hough transform.” *Computer Vision, Graphics, and Image Processing*, **44**(1):87–116, October 1988.
- [Jul71] B. Julesz. *Foundations of Cyclopean Perception*. University of Chicago Press, Chicago, 1971.
- [Kan54] Gaetano Kanizsa. “Il gradiente marginale come fattore dell’aspetto fenomenico dei colori.” *Archivio di Psicologia Neurologia e Psichiatria*, **15**(3), 1954.
- [Kan76] Gaetano Kanizsa. “Subjective Contours.” *Scientific American*, **234**(4):48–52, April 1976.

- [Kan79] Gaetano Kanizsa. *Organization in vision: Essays on Gestalt perception*. Praeger Publishers, New York, 1979.
- [Ken78] J. M. Kennedy. "Illusory contours and the ends of lines." *Perception*, 7(5):605–607, 1978.
- [KK89] L. A. Krubitzer and J. H. Kaas. "Cortical integration of parallel pathways in the visual system of primates." *Brain Research*, 478:161–165, 1989.
- [KNM84] S. W. Kuffler, J. G. Nicholls, and A. R. Martin. *From Neuron to Brain*. Sinauer Associates Inc., Sunderland, Massachusetts, second edition, 1984.
- [KWT87] Michael Kass, Andrew Witkin, and Demetri Terzopoulos. "Snakes: Active contour models." In *Proceedings of the First International Conference on Computer Vision*, Washington D. C., June 1987. IEEE Computer Society Press.
- [LH88] M. Livingstone and D. Hubel. "Segregation of Form, Color, Movement, and Depth: Anatomy, Physiology, and Perception." *Science*, 240:740–9, May 1988.
- [Mar82] D. Marr. *Vision: A Computational Investigation into the Human Representation and Processing of Visual Information*. Freeman, 1982.
- [MC91] B.S. Manjunath and R. Chellappa. "A unified approach to boundary perception: Edges, textures and illusory contours." Technical Report USC-SIPI Report No. 167, University of Southern California, 1991.
- [McC90] James D. McCafferty. *Human and Machine Vision: Computing Perceptual Organisation*. Ellis Horwood Limited, West Sussex, England, 1990.
- [Mes92] E. Mesrobian. *A Neural Network Model for Textural Segmentation*. PhD thesis, University of California, Los Angeles, Dept of Computer Science, 1992.
- [MP76] David Marr and Tomaso Poggio. "Cooperative computation of stereo disparity." *Science*, 194:283–287, 1976.
- [MS92] E. Mesrobian and J. Skrzypek. "A Software Environment for Studying Computational Neural Systems." *IEEE Transactions on Software Engineering*, 18(7):575–589, July 1992.

- [NS90] Ken Nakayama and Shinsuke Shimojo. "Da Vinci stereopsis: Depth and subjective occluding contours from unpaired image points." *Vision Research*, **30**(11):1811–1825, 1990.
- [NS92] Ken Nakayama and Shinsuke Shimojo. "Experiencing and perceiving visual surfaces." *Science*, **257**:1357–1363, September 1992.
- [NSS89] Ken Nakayama, Shinsuke Shimojo, and Gerald Silverman. "Stereoscopic depth: its relation to image segmentation, grouping, and the recognition of occluded objects." *Perception*, **18**:55–68, 1989.
- [ODF90] Izumi Ohzawa, Gregory DeAngelis, and Ralph Freeman. "Stereoscopic depth discrimination in the visual cortex: Neurons ideally suited as disparity detectors." *Science*, **249**:1037–1041, 1990.
- [Par89] Theodore Parks. "Illusory-figure lightness: Evidence for a two-component theory." *Perception*, **18**:783–788, 1989.
- [PC92a] Franco Purghe and Stanley Coren. "Amodal completion, depth stratification, and illusory figures: a test of Kanizsa's explanation." *Perception*, **21**:325–335, 1992.
- [PC92b] Franco Purghe and Stanley Coren. "Subjective Contours 1900-1990: Research trends and bibliography." *Perception & Psychophysics*, **51**(3):291–304, March 1992.
- [PH89] E. Peterhans and R. von der Heydt. "Mechanism of contour perception in monkey visual cortex. II. Contours bridging gaps." *The Journal of Neuroscience*, **9**(5):1749–1763, May 1989.
- [PH91] E. Peterhans and R. von der Heydt. "Elements of form perception in the monkey prestriate cortex." In *Representations of Vision*, pp. 111–124. Cambridge University Press, 1991.
- [PHB86] E. Peterhans, R. von der Heydt, and G. Baumgartner. "Neuronal responses to illusory contour stimuli reveal stages of visual cortical processing." In *Visual Neuroscience*, pp. 343–351, Cambridge, 1986. Cambridge University Press.
- [PM87] Susan Petry and Glenn E. Meyer. *The Perception of Illusory Contours*. Springer-Verlag, New York, 1987.
- [PN91] Michael A. Paradiso and Ken Nakayama. "Brightness perception and filling-in." *Vision Research*, **31**(7/8):1221–1236, 1991.

- [Pra85] K. Prazdny. "On the nature of inducing forms generating perceptions of illusory contours." *Perception & Psychophysics*, **37**(3):237–242, March 1985.
- [PSN89] Michael A. Paradiso, Shinsuke Shimojo, and Ken Nakayama. "Subjective contours, tilt aftereffects, and visual cortical organization." *Vision Research*, **29**(9):1205–1213, 1989.
- [PTK85] Tomaso Poggio, Vincent Torres, and Christof Koch. "Computational vision and regularization theory." *Nature*, **317**(6035):314–319, September 1985.
- [Ram85a] V. S. Ramachandran. "Apparent motion of subjective surfaces." *Perception*, **14**(2):127–134, 1985.
- [Ram85b] V. S. Ramachandran. "The neurobiology of perception." *Perception*, **14**(2):97–103, 1985.
- [Ram86] V. S. Ramachandran. "Capture of stereopsis and apparent motion by illusory contours." *Perception & Psychophysics*, **39**(5):361–373, May 1986.
- [Ram87] V. S. Ramachandran. "Visual perception of surfaces: A biological theory." In *The Perception of Illusory Contours*, pp. 91–108. Springer-Verlag, 1987.
- [RCC86] C. Redies, J. M. Crook, and O. D. Creutzfeldt. "Neuronal responses to borders with and without luminance gradients in cat visual cortex and dorsal lateral geniculate nucleus." *Experimental Brain Research*, **61**(3):469–481, 1986.
- [RG91] V. S. Ramachandran and R. L. Gregory. "Perceptual filling in of artificially induced scotomas in human vision." *Nature*, **350**(6320):699–702, April 1991.
- [RHW85] D.E. Rumelhart, G.E. Hinton, and R.J. Williams. "Learning Internal Representations By Error Propagation." Technical Report ICS Report 8506, Institute For Cognitive Science, University of California, San Diego, 1985.
- [RS91] B. Ringer and J. Skrzypek. "A Neural Architecture for Illusory Contour Detection." Technical Report UCLA-MPL-TR 91-8, Machine Perception Laboratory, University of California, Los Angeles, 1991.

- [Rub58] E. Rubin. "Figure and ground." In *Readings in Perception*. Van Nostrand Press, 1958.
- [Sab85] Daniel Sabbah. "Computing with connections in visual recognition of origami objects." *Cognitive Science*, **9**:25–50, January–March 1985.
- [Sch04] F. Schumann. "Einige Beobachtungen Uber die Zusammenfassung von Gesichtseindruckern zu Binheiten." *Psychologische Studien*, **1**:1–32, 1904.
- [SG85] Robert Shapley and James Gordon. "Nonlinearity in the perception of form." *Perception & Psychophysics*, **37**(1):84–88, January 1985.
- [SG87] Robert Shapley and James Gordon. "The existence of interpolated contours depends on contrast and spatial separation." In *The Perception of Illusory Contours*, pp. 109–115. Springer-Verlag, 1987.
- [SG92] J. Skrzypek and D. Gungner. "Lightness constancy from luminance contrast." *International Journal of Pattern Recognition and Artificial Intelligence*, **6**(1):1–36, 1992.
- [SHH87] Jeff Shrager, Tad Hogg, and Bernardo A. Huberman. "Observations of phase transitions in spreading activation networks." *Science*, **236**:1092–1094, 1987.
- [SK90] Thomas F. Shipley and Philip J. Kellman. "The role of discontinuities in the perception of subjective figures." *Perception & Psychophysics*, **48**(3):259–270, 1990.
- [SM91] J. Skrzypek and E. Mesrobian. "A connectionist architecture for textural segmentation of natural images." In *Proceedings of MICRO-91 (Microelectronics Innovation and Computer Research)*, UCSD San Diego, California, May 1991.
- [SN90] Shinsuke Shimojo and Ken Nakayama. "Amodal representation of occluded surfaces: role of invisible stimuli in apparent motion correspondance." *Perception*, **19**(3):285–299, March 1990.
- [SO75] Andrew Smith and Ray Over. "Tilt aftereffects with subjective contours." *Nature*, **257**(5527):581–582, October 1975.
- [SR92a] J. Skrzypek and B. Ringer. "Illusory Contours and Image Segmentation; Neural Network Architectures." In Omid M. Omidvar, editor,

Progress in Neural Networks, volume IV. Ablex Publishing Corporation, 1992. in press.

- [SR92b] J. Skrzypek and B. Ringer. "Neural network models for illusory contours perception." In *Proceedings of IEEE Computer Vision and Pattern Recognition*, New York, 1992. IEEE Press.
- [SSN89] Shinsuke Shimojo, Gerald H. Silverman, and Ken Nakayama. "Occlusion and the solution to the aperture problem for motion." *Vision Research*, **29**(5):619–626, 1989.
- [Ull76] S. Ullman. "Filling-in the Gaps: The shape of subjective contours and a model for their generation." *Biological Cybernetics*, **25**(1):1–6, 1976.
- [VDO89] D. C. Van Essen, E. A. DeYoe, J. F. Olavarria, J. J. Knierim, J. M. Fox, D. Sagi, and B. Julesz. *Neuronal Responses to Static and Moving Texture Patterns in Visual Cortex of the Macaque Monkey*, chapter 6, pp. 137–154. Portfolio Publishing, Woodlands, Texas, 1989.
- [VO87] Rufin Vogels and Guy A. Orban. "Illusory contour orientation discrimination." *Vision Research*, **27**(3):453–467, 1987.
- [VOL90] Mark Versavel, Guy Orban, and Lieven Lagae. "Responses of visual cortical neurons to curved stimuli and chevrons." *Vision Research*, **30**(2):235–248, 1990.
- [WR89] Hugh Wilson and Whitman A. Richards. "Mechanisms of contour curvature discrimination." *Journal of Optic Society of America*, **6**(1):106–115, January 1989.
- [WS88] Hans Wallach and Virginia Slaughter. "The role of memory in perceiving subjective contours." *Perception & Psychophysics*, **43**(2):101–106, February 1988.
- [You86] R. A. Young. "The Gaussian Derivative Model for Machine Vision: Visual Cortex Simulation." Technical Report GMR-5323, General Motors Research Laboratories, 1986.
- [You91] Richard A. Young. "Oh say, can you see? The physiology of vision." In *SPIE Proceedings, San Jose, California*, 1991.
- [ZS88] S. Zeki and S. Shipp. "The functional logic of cortical connections." *Nature*, **335**(22):311–317, 1988.